Supplementary Materials for

Non-equilibrium plasma co-upcycling of waste plastics and CO_2 for carbon-negative oleochemicals

Harish Radhakrishnan ‡[a], Samirah Gnangbe ‡[a], Alif Duereh[a], Sultan Ul Iffat Uday[a], Lusi A[a], Haiyang Hu [b], Hui Hu[b], Mark Mba Wright*[a], Xianglan Bai*[ac]

[a] Department of Mechanical Engineering, Iowa State University, Ames, IA, 50011, USA

[b] Department of Aerospace Engineering, Iowa State University, Ames, IA, 50011, USA

[c] Department of Chemical & Biological Engineering, Iowa State University, Ames, IA, 50011, USA

‡ Co-first authors

* Corresponding authors

This PDF file includes:

Supplementary Text

- Section A: Additional materials
- Section B: NMR-based functional group selectivity
- Section C: Isotopic CO_2 plasma-based model compound conversion
- Section D: Methodology for techno-economic and lifecycle assessment
- Section E: Additional results for techno-economic and lifecycle assessment

Figs. S1 to S23

Tables S1 to S12

Equations S1 to S4

Supplementary References: 1 to 27

Supplementary Text

Section A: Additional materials

The standard calibration chemicals are listed below.

Alkane standard chemicals

- Saturated alkanes (C_7-C_{40}) standard (Sigma-Aldrich)
- Hexane (Sigma Aldrich)
- Dodecane (Sigma Aldrich)
- Octadecane (Sigma Aldrich)
- Eicosane (Fisher Scientific)
- Tetradecane (Fisher Scientific)

Alkene standard chemicals

- 1-Pentene (Sigma-Aldrich)
- 1-Hexene (TCI America)
- 1-Heptene (Thermo Scientific)
- 1-Octene (TCI America)
- 1-Nonene (Sigma-Aldrich)
- 1-Decene (TCI America)
- 1-Undecene (Thermo Scientific)
- 1-Dodecene (TCI America)
- 1-Tridecene (Thermo Scientific)
- 1-Tetradecene (TCI America)
- 1-Pentadecene (Thermo Scientific)
- 1-Hexadecene (TCI America)
- 1-Heptadecene (Thermo Scientific)
- 1-Octadecene (TCI America)
- 1-Nonadecene (Thermo Scientific)
- 1-Eicosene (TCI America)

- 1-Heneicosene (TCI America)
- 1-Docosene (TCI America)
- cis-9-Tricosene (TCI America)

Diene standard chemicals

- 1,5-Hexadiene (Thermo Scientific)
- 1,6-Heptadiene (Thermo Scientific)
- 1,7-Octadiene (Thermo Scientific)
- 1,8-Nonadiene (Thermo Scientific)
- 1,9-Decadiene (Thermo Scientific)
- 1,10-Undecadiene (Thermo Scientific)
- 1,11-Dodecadiene (Thermo Scientific)
- 1,13-Tetradecadiene (Thermo Scientific)

Carboxylic acid standard chemicals

- Pentanoic acid (Sigma Aldrich)
- Hexanoic acid (TCI America)
- Heptanoic acid (Sigma Aldrich)
- Octanoic acid (TCI America)
- Nonanoic acid (Sigma Aldrich)
- Decanoic acid (TCI America)
- Undecanoic acid (Sigma Aldrich)
- Dodecanoic acid (TCI America)
- Tridecanoic acid (Sigma Aldrich)
- Tetradecanoic acid (TCI America)
- Hexadecanoic acid (TCI America)
- Heptadecanoic acid (Thermo Scientific)
- Octadecanoic acid (TCI America)
- Nonadecanoic acid (Thermo Scientific)
- Eicosanoic acid (TCI America)

- Heneicosanoic acid (Thermo Scientific)
- Docosanoic acid (TCI America)
- Tetracosanoic acid (Sigma Aldrich)

Alcohol standard chemicals

- 1-Hexanol (Sigma Aldrich)
- 1-Heptanol (Sigma Aldrich)
- 1-Octanol (Sigma Aldrich)
- 1-Nonanol (Sigma Aldrich)
- 1-Decanol (Sigma Aldrich)
- 1-Dodecanol (Sigma Aldrich)
- 1-Tetradecanol (Sigma Aldrich)
- 1-Hexadecanol (Sigma Aldrich)
- 1-Octadecanol (Sigma Aldrich)
- 1-Eicosanol (Sigma Aldrich)
- 1-Heneicosanol (Thermo Scientific)
- 1-1-Docosanol (Sigma Aldrich)
- 1-Tetracosanol (Sigma Aldrich)
- 1-Hexacosanol (Sigma Aldrich)
- 1-Heptacosanol (Sigma Aldrich)
- 1-Octacosanol (Sigma Aldrich)
- 1-Triacontanol (Sigma Aldrich)

Diol standard chemicals

- 1,5-Pentanediol (Thermo Scientific)
- 1,6-Hexanediol (Thermo Scientific)
- 1,8-Octanediol (Thermo Scientific)
- 1,9-Nonanediol (Thermo Scientific)
- 1,10-Decanediol (Thermo Scientific)
- 1,12-Dodecanediol (Thermo Scientific)

Carbonyl standard chemicals

- Hexanal (Thermo Scientific)
- Heptaldehyde (Sigma Aldrich)
- Octanal (Sigma Aldrich)
- Nonanal (Thermo Scientific)
- Decanal (TCI America)
- Undecanal (Thermo Scientific)
- Dodecanal (TCI America)
- Tridecanal (TCI America)
- Tetradecanal (TCI America)
- Pentadecanal (TCI America)
- Hexadecanal (TCI America)
- Heptadecanal (TCI America)
- Octadecanal (TCI America)

Section B: NMR-based functional group selectivity analysis

The selectivity of functional groups was calculated using the following equations adapted from the methods specified in literature[1-3]. The peak areas of the carbons linked to the different functional groups in the liquid product are denoted by [A], [B], [C], [D], and [E], where

[A] = peak area of R-$\underline{C}H_2$-OH (assigned 60-95 ppm),

[B] = peak area of R-$\underline{C}$OOH (assigned 175-180 ppm),

[C] = peak area of R-$\underline{C}$OH, R-$\underline{C}$O-R' and R-$\underline{C}$OO-R' (assigned 180-210 ppm),

[D] = average of peak areas of R-$\underline{C}$H=CH_2 (assigned 135-140 ppm) and R-CH=$\underline{C}H_2$ (assigned 110-115 ppm), and

[E] = peak area of R-$\underline{C}H_3$ (assigned 10-20 ppm).

The ^{13}C-NMR selectivity of the different functional groups was calculated as follows:

$$\text{Alcohols [F]} = \frac{[A]}{[A]+[B]+[C]+[D]+[E]-([A]+[B]+[C]+[D])/2} \times 100\%$$

$$\text{Carboxylic acids [G]} = \frac{[B]}{[A]+[B]+[C]+[D]+[E]-([A]+[B]+[C]+[D])/2} \times 100\%$$

$$\text{Other oxygenated compounds [H]} = \frac{[C]}{[A]+[B]+[C]+[D]+[E]-([A]+[B]+[C]+[D])/2]} \times 100\%$$

$$\text{Olefins [I]} = \frac{[D]}{[A]+[B]+[C]+[D]+[E]-([A]+[B]+[C]+[D])/2]} \times 100\%$$

$$\text{Paraffins [J]} = \frac{[E]-([A]+[B]+[C]+[D])/2}{[A]+[B]+[C]+[D]+[E]-([A]+[B]+[C]+[D])/2} \times 100\%$$

$$\text{Aliphatic hydrocarbons [K]} = [I] + [J]$$

Section C: Isotopic CO_2 plasma-based model compound conversion

CO_2-based plasma conversion of eicosane was carried out using $^{13}CO_2$ to distinguish between CO_2-originated and plastic-originated carbons in the product. The model compound was also converted using regular $^{12}CO_2$ plasma to aid product identification in GC/MS. The number of CO_2-originated carbons and their possible positions in a molecule was determined by comparing the mass-to-charge ratio (*m/z*) of the $^{13}CO_2$ plasma-based molecule in its mass spectra (MS) and that of the corresponding regular molecule obtained using either regular CO_2 plasma or NIST library database. When one ^{12}C atom in a molecule having *m/z* = M is substituted by one ^{13}C atom, it will cause an increase of the *m/z* value by one mass unit (*m/z* = M+1).

In this work, ^{13}C carbons were observed in product compounds with four different functional groups (e.g., hydrocarbon, alcohol, carboxylic acid, and carbonyl). The results are discussed below using representative compounds found in liquid product analysis.

Hydrocarbon. Fig. S7 shows the *m/z* distribution of 5-octadecene obtained with $^{13}CO_2$ plasma (upper) compared to the regular compound (lower). The molecular peak ion of regular 5-octadecene has an *m/z* value of 252, whereas the compound obtained with $^{13}CO_2$ plasma exhibited three *m/z* peaks at 253, 254, and 255. These results indicated that up to three carbons in the olefin were substituted by CO_2-originated carbons. The additional fragment peaks of alkyl ions at *m/z* 69 to 72 were also detected in the compound based on $^{13}CO_2$ plasma. These results can be used to locate the position of ^{13}C atoms being replaced, where three ^{13}C atoms are expected to be at the chain end of the molecule.

Alcohol. Fig. S8 shows mass spectra of allyl alcohol, trimethylsilyl (TMS) derivative compared between the $^{13}CO_2$ plasma case (upper) and regular $^{12}CO_2$ plasma case (lower). In this work, the compound was silylated by TMS to detect and increase the GC signals of alcohol and carboxylic acid compounds. The H atom in both compounds is substituted by trimethylsilyl ($-Si-(CH_3)_3$). The regular allyl alcohol showed the *m/z* value at 130, whereas the *m/z* value of the $^{13}CO_2$ plasma-based compound appeared at 133. These results indicated that the alcohol could contain up to three CO_2-originated carbon atoms.

Carboxylic acid. Fig. S9 shows the mass spectra of palmitic acid, TMS derivative compared between the $^{13}CO_2$ plasma-based compound (upper) and regular compound (lower). Both spectra

showed *m/z* values at 328 (final mass ion), 329 (M+1), and 330 (M+2). The presence of ^{13}C atoms in nature causes the extra MS peaks to appear in the regular compound. When the relative *m/z* peak intensity ratios at 329 to 328 and 330 to 328 are considered, both ratios for the $^{13}CO_2$ plasma-based compound (Entry 5-6, **Table S6**) are higher than those for the regular compound. These results implied that the compound contains up to two CO_2-originated carbon atoms.

The fragment peaks were also considered to locate the position of the ^{13}C atoms in the molecule. Both spectra (**Fig. S9**) exhibited strong peak signals at *m/z* 313 due to fragment cleavage of methyl groups (M-15). The relative *m/z* peak intensity ratios at 314 to 313 and 315 to 313 (Entry 3-4, **Table S6**) are the same for both spectra, indicating that one ^{13}C atom is located at the chain end of the molecular structure. Another ^{13}C atom is possibly located at the carboxylic functional groups, according to the fragment of the silylated carboxylic groups (-C=O-O-Si-$(CH_3)_3$) at *m/z* 117. Both *m/z* intensity ratios of 118 to 117 and 119 to 117 (Entry 1-2, **Table S6**) for the $^{13}CO_2$-based compound are higher than those for the regular compound. We also evaluated an additional carboxylic compound (arachidonic acid) to confirm these results, as shown in **Fig. S10**. It was found that both ratios for the $^{13}CO_2$-based compound (Entry 7-8, **Table S6**) are also higher than those of the corresponding regular compound.

Carbonyl. Fig. S11 shows the mass spectra of 9-octadecanone compared between the $^{13}CO_2$ plasma-based case (upper) and regular case (lower). Since the final *m/z* of 268 was not shown in both spectra, the fragments of 9-octadecanone were evaluated. Both spectra (**Fig. S11**) exhibited strong peak signals at *m/z* 141 due to fragments of alkyl ion $(C_{10}H_{21})^+$ and acyl ion $(C_9H_{17}O)^+$. While the regular compound showed one extra *m/z* peak at 142, the $^{13}CO_2$ plasma-based compound showed two extra *m/z* peaks at 142 and 143. In addition, the relative *m/z* peak intensity ratios of $^{13}CO_2$ plasma-based compound spectra at 142/141 and 143/141 (**Table S7**) are higher than those of the regular compound. These results implied the molecule could contain up to two CO_2-originated carbon atoms.

Section D: Methodology for techno-economic and lifecycle assessment

Process modeling

A conceptual facility was designed for a processing capacity of 200 metric tons (MT) of waste PE/day, which is the daily average amount of plastic waste delivered to Material Recovery Facilities[4]. The process was modeled with the open-source platform BioSteam 2.38.6[5] based on lab-scale experimental results. Two scenarios, which are based on cases Q and R results in this work by converting PC-PE, using different plasma gas compositions, were considered in the study:

- Scenario 1 (case Q) – CO_2 plasma: 77.2% Post-consumer PE, 22.8% CO_2, and 0% O_2
- Scenario 2 (case R) – CO_2/O_2 plasma: 73.6% Post-consumer PE, 16.5% CO_2, and 9.9% O_2

The process design consists of three major processing areas, which are discussed below and depicted in **Fig. S15.**

Plasma reaction (A100). The process model begins by feeding PE into the dielectric barrier discharge (DBD) plasma reactor. The plasma carrier gas can be pure CO_2 or CO_2/O_2 mixture gas, depending on the scenario. The plasma reactor operates at atmospheric pressure and ambient temperature. The energy required to run the plasma reactor was determined from Equation (S1).

$$Power\ \left(\frac{MJ}{kg}\right) = 0.2408 * feedrate(\frac{kg}{s})^{0.234} \quad \text{(S1)}$$

Equation (S2) was derived by fitting a power-law model to reported values of plasma power in the literature[6]. The model was validated by experimental observations. The plasma power consumption as a function of the reactor feed rate is shown in **Fig. S16.** The literature shows a rapid decrease in the power consumed per material unit as the feed rate increases. This reduction is attributed to decreased energy losses to the environment as the reactor size increases and more material is available to capture the heat. When oxygen is introduced into the plasma reactor, the energy required decreases due to the additional heat supplied by the oxidation reaction. To account for this reduction in power, a factor of 0.8 is added to Equation (S2) for CO_2/O_2 plasma, which also agrees with experimental observation **(Table S1)**.

The exit temperature of the plasma vapor product is set at 350 °C based on experimental results given in **Table S1**, which then goes through condensation. The non-condensable gases (NCGs), which consist of CO_2, CO, H_2, and C_1-C_5 gases are collected downstream. CO_2 is recycled to the plasma reactor and the other gases are combusted to generate power and heat in the facility.

Product fractionation and recovery (A200). For the liquid product separation, C_5-C_{12} hydrocarbons are collected as olefins, C_{13}-C_{20} are collected as paraffin, C_{11}-C_{20} alcohols are collected as fatty alcohols, C_{11}-C_{20} acids are collected as fatty acids, and C_{12}-C_{20} carbonyls are collected as fatty aldehydes. The compounds were separated using fractional distillation and distillation columns based on their boiling points. The average boiling points of olefins, paraffin, fatty alcohols, fatty acids, and carbonyls were 391.35 K, 589.15 K, 537.25 K, 546.15 K, and 552.15 K respectively.

The oxygenated liquid product obtained from the plasma reaction is cooled and condensed at 32 ℃, then, it enters a flash separator, operating at 200 ℃, where C_1-C_{12} compounds are vaporized and separated from C_{12+} liquid compounds. The liquid oil is sent to a distillation column to separate C_{12}-C_{20} compounds with 98% recovery, while the heavy C_{20+} oil stream is sent to A300 for power production. The C_1-C_{12} gaseous mixture from the flash separator is compressed to 4 bar and cooled to -78 ℃ to separate CO_2, CO, H_2, and other light C_1-C_4 hydrocarbons through a cryogenic process involving a series of compression and cooling phases. CO_2 and 10% of the recovered gases, mentioned above, is recycled into the plasma reactor to enhance the conversion efficiency while the remaining gases are sent to the power generation unit.

The C_5-C_{12} compounds are heated to 2 ℃ and compressed to 25 bar. A de-olefinizer column unit separates C_5-C_{12} olefins from the oxygenated liquid. The distillate from the de-olefinizer is further purified in a fractionator to separate the olefins from other compounds in the stream. The bottom liquid product of the de-olefinizer unit is mixed with the distillate C_{12}-C_{20} compounds. This mixture is sent to the alcohol separator where C_{11}-C_{20} alcohol and acid products are recovered overhead. This distillate is heated, compressed, and sent to the alcohol column to collect fatty alcohols. The bottom product from this column is sent to a second column where fatty acids are recovered.

The bottom of the alcohol separator is sent to a distillation column where carbonyls (fatty aldehydes) are recovered. The heavy keys of the carbonyl column are sent to the paraffin columns, where paraffins are recovered in the distillate. The bottom of the paraffin column is sent to A300 for heat and power generation.

Heat and power systems (A300). C_{20+} compounds, bottoms or distillate of the compounds columns, and 90% of the non-CO_2 gas yield are fed to the boiler turbogenerator system. The boiler

and generator mechanical efficiencies are assumed to be 80% and 85%, respectively. The power and heat generated are used to cover the energy requirements of the plant, and the rest is sold to the grid.

Techno-economic analysis

The study employs techno-economic analysis (TEA) to evaluate the economic performance of the two scenarios. The capital cost and operation cost of the plant were first determined and incorporated into the discounted cash flow analysis, which yielded the net present value (NPV) and internal rate of return (IRR) of each scenario. The NPV and IRR are profitability metrics by which each process scenario can be effectively compared.

Financial assumptions. The economic analysis reported in this study is based on the n^{th} plant assumption. The n^{th} plant economic indicates that similar technologies have already been built and are commercially available[7-9]. A summary of the n^{th} plant assumption is presented in **Table S9**. These economic assumptions made in the study are consistent with assumptions used in other TEA reports on plastic upcycling[10-12]. The analysis assumes that the plant would be 40% equity financed, and the remaining 60% will be financed at a 7% interest rate and a 10-year term of repayment. For the estimation of the NPV, the IRR was set at 10% for 20 years of the plant's lifetime. The capital depreciation is based on the Modified Accelerated Cost Recovery System (MACRS) for a 7-year recovery period. The study assumed an income tax rate of 21%, a construction period of 24 months, and a startup time of 6 months.

Capital cost estimation. Capital cost is the summation of the fixed capital investment (FCI) and the working capital cost. The FCI consists of the total direct cost (TDC) and the indirect capital cost (IDC). The TDC refers to the expenses required for the construction of the facility, which includes the cost of purchasing equipment, piping, installation, buildings, and other related costs. The IDC are non-construction expenses usually related to project management, engineering design, licenses, and permits.

The cost for the majority of the equipment was derived from the NREL report by Humbird et al.[12]. Costs for common process equipment, such as heat exchangers, compressors, and distillation columns, were obtained from BioSteam. The equipment cost reported in the literature is specific to the production capacity, which may differ from this process. Therefore, an exponential scaling

must be employed to adjust the purchase equipment costs to the actual capacity of this process using Equation S2:

$$Equipment\ cost = Base\ Equipment\ Cost\left(\frac{Design\ capacity}{Base\ Capacity}\right)^{n} \quad \text{(S2)}$$

In this equation, n is the characteristic scaling exponent that can vary from 0.6 to 1 based on the process equipment. The design capacity is determined from the material and energy balance from the process model. The fixed capital cost was determined by multiplying the equipment cost with a Lang factor using Equation S3. The LANG factor typically ranges from 2 to 5 depending on the technology, process design detail, and other factors. The lower end of the range is typical for liquid chemical facilities. In this article, a LANG factor of 5 was used for a conservative estimate (i.e., a higher capital cost).

$$FCI = F_{Lang} \ * \ Purchased\ Equipment\ Cost \quad \text{(S3)}$$

The working capital was assumed to be 5% of the FCI, covering start-up expenses like raw materials and utilities. In addition, it was assumed that there would be no revenue from selling the plant facilities after its lifetime.

Operating cost estimation. Operating costs consist of the total variable production cost, fixed charges, and overhead costs, as shown in **Table S10**. The cost of the PE waste was assumed at \$25/ton, which includes the waste handling, transportation, and pretreatment expenses[10,13]. The average cost of CO_2 is assumed at \$35/MT, employed in previous studies on CO_2 utilization processes[14,15]. The utility usage was evaluated based on the mass and energy balance in BioSteam, and the costs were acquired from literature and online databases[16,18]. Electricity and heat are generated in the facility, and the excess energy is sold to the grid. The labor requirement was estimated based on the NREL report by Humbird et al.[12], tabulated in **Table S10.** In this process, revenue was generated from the sales of the products and excess electricity and heat. The current market price of olefins, fatty alcohols, fatty acids, paraffins, and carbonyls (fatty aldehydes) were obtained from online databases[19-23].

Profitability analysis. The economic performance of the scenarios was evaluated using the profitability indicators NPV and IRR. The NPV determines the profitability of the facility over its lifetime. This is done by discounting future cash flows to their present value. A positive NPV indicates the process's profitability, while a negative NPV suggests the opposite. Equation (S4) defines the NPV.

$$NPV = \sum_{t=1}^{T} \frac{I_t}{(1+d)^t} - I_0 \quad \text{(S4)}$$

In this equation, t is the plant lifetime in years, I_0 is the initial investment, I_t is the net cash flow during period t, and d is the discount rate. The IRR is an essential economic metric for assessing the effectiveness of the investment and directly comparing the two scenarios. It represents the discount rate at which the NPV becomes zero, which can be calculated from Equation S4. The minimum selling price (MSP) of the product with the highest yield was calculated from the discount cash flow at an IRR of 10% over a 20-year lifetime.

Sensitivity analysis was conducted to evaluate the impact of changes in the baseline cost of capital investment, plastic and other feedstock prices, plasma energy, and product prices on the plant's economy. Specifically, a 20% change in each factor is analyzed to determine the potential effect on the plant's net present value.

Lifecycle assessment

Life Cycle Assessment (LCA) is a reliable and comprehensive method to assess and quantify the environmental sustainability of a given process or product throughout its entire life cycle. LCA allows for identifying and improving the potential environmental impacts of a product, starting from the acquisition of raw materials through production and usage to the final disposal stage. This study utilized LCA to evaluate the environmental and human health impact of producing chemicals from the non-thermal plasma deconstruction of plastic waste. The analysis was performed in OpenLCA 1.11.0[24] and the EcoInvent database, using the Tool for Reduction and Assessment of Chemicals and Other Environmental Impacts (TRACI) as the impact assessment method. The system boundary used for the LCA is shown in **Fig. S17**, which involves the product manufacturing processes. We assume a zero-burden emission for the plastic waste, which implies that any impacts associated with the production, collection, and treatment of the waste PE are attributed to the suppliers[25]. In addition, the impacts associated with the CO_2 feedstock are also

attributed to the CO_2 point source[14]. The study applied a functional unit of 1 kg of plastic waste processed in the plant, facilitating the comparison across the different scenarios. This process produces various platform chemicals, as well as excess heat and electricity. Therefore, in the analysis, all the products are assumed to substitute similar products from petroleum processes, resulting in credits earned. The life cycle inventory list of the inputs and outputs is presented in **Table S11.** For each scenario, the analysis considers cases where the facility power consumption is generated by wind power, and the production of power and heat from the on-site combustion of the flue gases displace grid electricity.

Section E: Additional results for techno-economic and lifecycle assessment

Material and energy balances. Figs. S18 and S19 show the mass and energy flows of a 200 tonnes per day (tpd) plastic waste plant for scenario 1 (CO_2 plasma) and scenario 2 (CO_2/O_2 plasma). The energy yield in the process was calculated based on the high heating value. Plastic is the primary energy input of the plant, accounting for 341.14 GJ/hr. For the CO_2 plasma scenario, the plant produces 332.5 GJ/hr of chemicals and 61.95 GJ/hr of power and heat, and the chemicals mass yield is 75.5%. For the CO_2/O_2 plasma plant, 78.85 GJ/hr of energy is produced with 328.8 GJ/hr of chemicals, and the chemicals mass yield is 71.1%.

In both scenarios, the yield of fatty alcohol is the highest, accounting for more than 37% and 50% of the inputs for scenario 1 and scenario 2, respectively. The electricity generated is used to power the plasma reactor, compressors, distillation columns, and other components. The energy produced covers all the plant's energy requirements, and the excess is sold to the grid.

The plasma power was determined using a power law regression to literature data shown in Equation S1. The plasma power consumption of the CO_2 plasma and CO_2/O_2 plasma is respectively 0.111 kW and 0.08 kW. Non-thermal plasma reactions are energy efficient and do not require excessive heating, unlike other thermochemical recycling methods.

Techno-economic analysis. Fig. S20 shows the total equipment installed cost (TIC) for the two scenarios**.** The TIC for scenarios 1 and 2 is $52.7 million and $56.9 million, respectively. **Fig. S21** shows the operating parameters used in the calculation of the MSP. **Fig. S22** presents the outcomes of the sensitivity analysis carried out on the scenarios**.** The sensitivity analysis results

show that the capital cost and alcohol price have the most significant impact on the NPV, whereas the feedstock price and plasma energy consumption have a limited effect on it.

Lifecycle assessment. The LCA of the production of chemicals from plastic waste was performed by accounting for the material and energy inputs from process simulation and their environmental impacts. **Table S12** shows the environmental impacts of each scenario. The scenarios include a comparison with using wind power instead of on-site energy generation. Thus, there are four scenarios:

Scenario 1: PC-PE conversion by CO_2 plasma using on-site energy generation

Scenario 2: PC-PE conversion by CO_2/O_2 plasma on-site energy generation

Scenario 3: PC-PE conversion by CO_2 plasma using wind electricity

Scenario 4: PC-PE conversion by CO_2/O_2 plasma using wind electricity

In general, these impacts are a small fraction of the impacts from producing fossil-based alternatives. In addition to producing chemicals, the process generates excess heat and electricity. It is assumed that any excess heat and electricity would be sold to the grid, resulting in coproduct credits for the avoided greenhouse gas emissions of fossil energy consumption. The GWP for all four scenarios ranges from -3.33 to -3.07 $kgCO_2e/kg$ PE. All scenarios resulted in negative emissions as the credits obtained from the products exceeded the emissions generated in the process. The carbon emissions from the combustion of flue gases in the boiler turbo-generator are the main positive contributor to the increase of GWP. Scenarios 3 and 4, where the electricity is supplied by wind energy, slightly decrease the GWP because of the additional credits obtained from selling all the energy produced from the on-site gas combustion. Scenario 4 has the lowest GWP of -3.33 $kgCO_2e/kg$ PE due to the high credits obtained from producing a larger amount of fatty alcohols. Scenario 2 and scenario 4 have positive indicators in eutrophication, ozone depletion, photochemical oxidation, and carcinogenic because of the addition of oxygen in the plasma reactor.

The sensitivity analysis was performed for the LCA by varying ±20% heat, electricity, and chemical products on the GWP. The results presented in **Fig. S23** show that alcohols, electricity, heat, and olefins significantly contribute to global warming potential.

Supplementary Figures

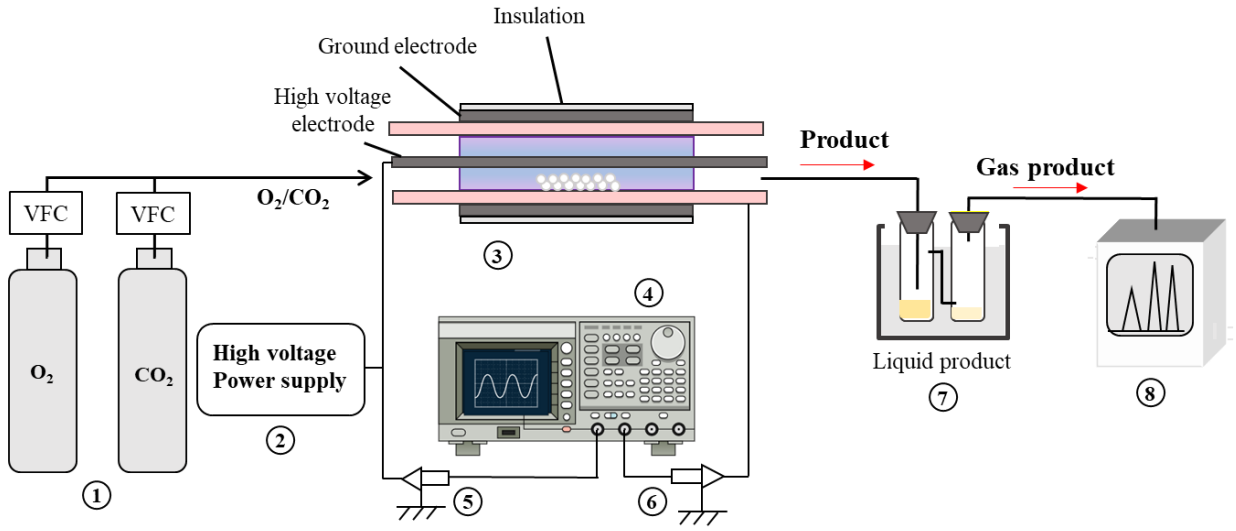

Figure S1. Schematic diagram of plasma-based conversion system setup. 1- gas cylinders; 2- high-voltage plasma power supply; 3- plasma reactor; 4 - oscilloscope; 5- high-voltage probe; 6- current probe; 7 - condenser; and 8- micro-GC

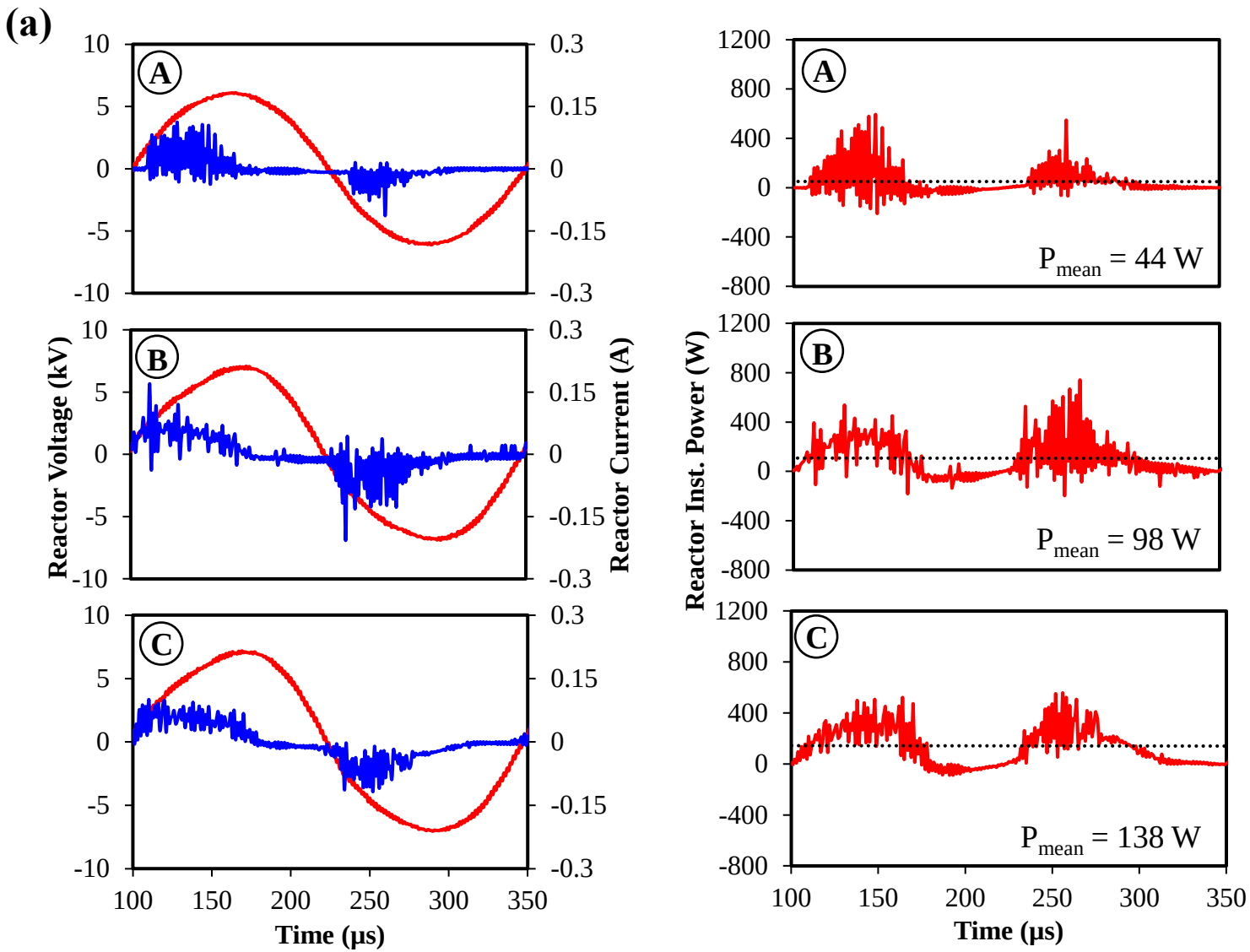
(a)
A
B
C
Reactor Voltage (kV)
Reactor Current (A)
Reactor Inst. Power (W)
Time (μs)
P mean = 44 W
P mean = 98 W
P mean = 138 W

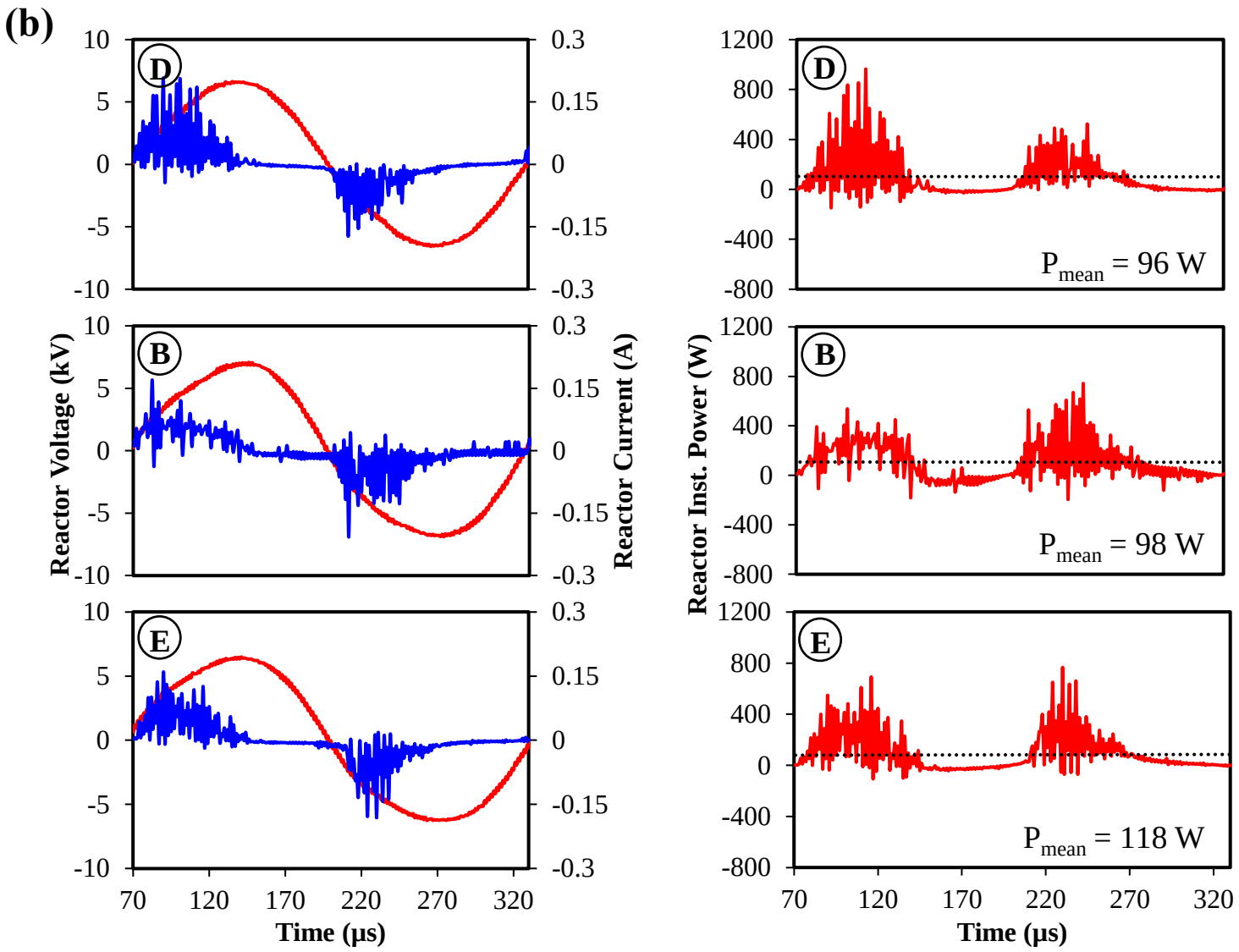
(b)
D
B
E
Reactor Voltage (kV)
Reactor Current (A)
Reactor Inst. Power (W)
Time (µs)
P mean = 96 W
P mean = 98 W
P mean = 118 W

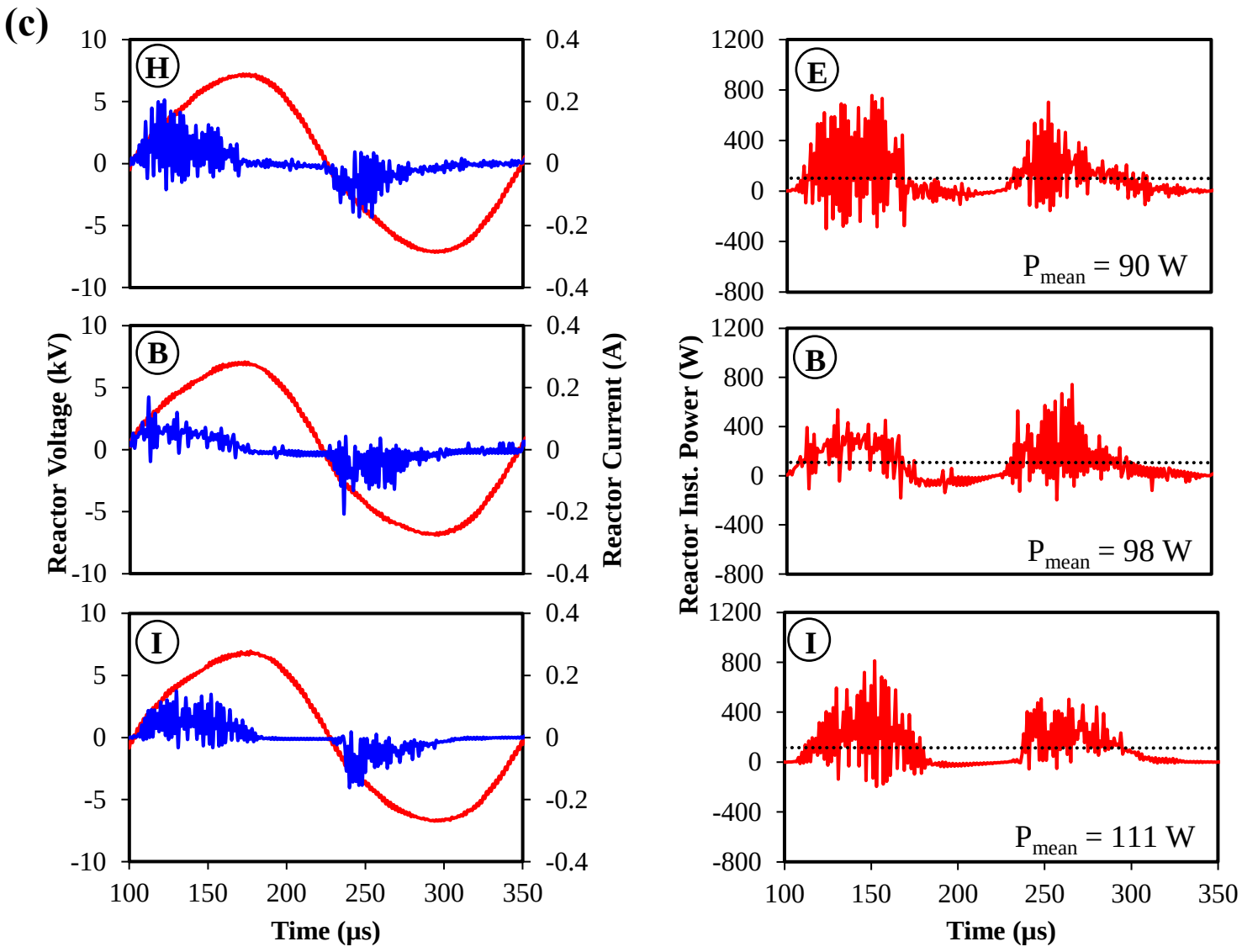
(c)
H
B
I
E
B
I
Reactor Voltage (kV)
Reactor Current (A)
Reactor Inst. Power (W)
Time (µs)
Time (µs)
P mean = 90 W
P mean = 98 W
P mean = 111 W

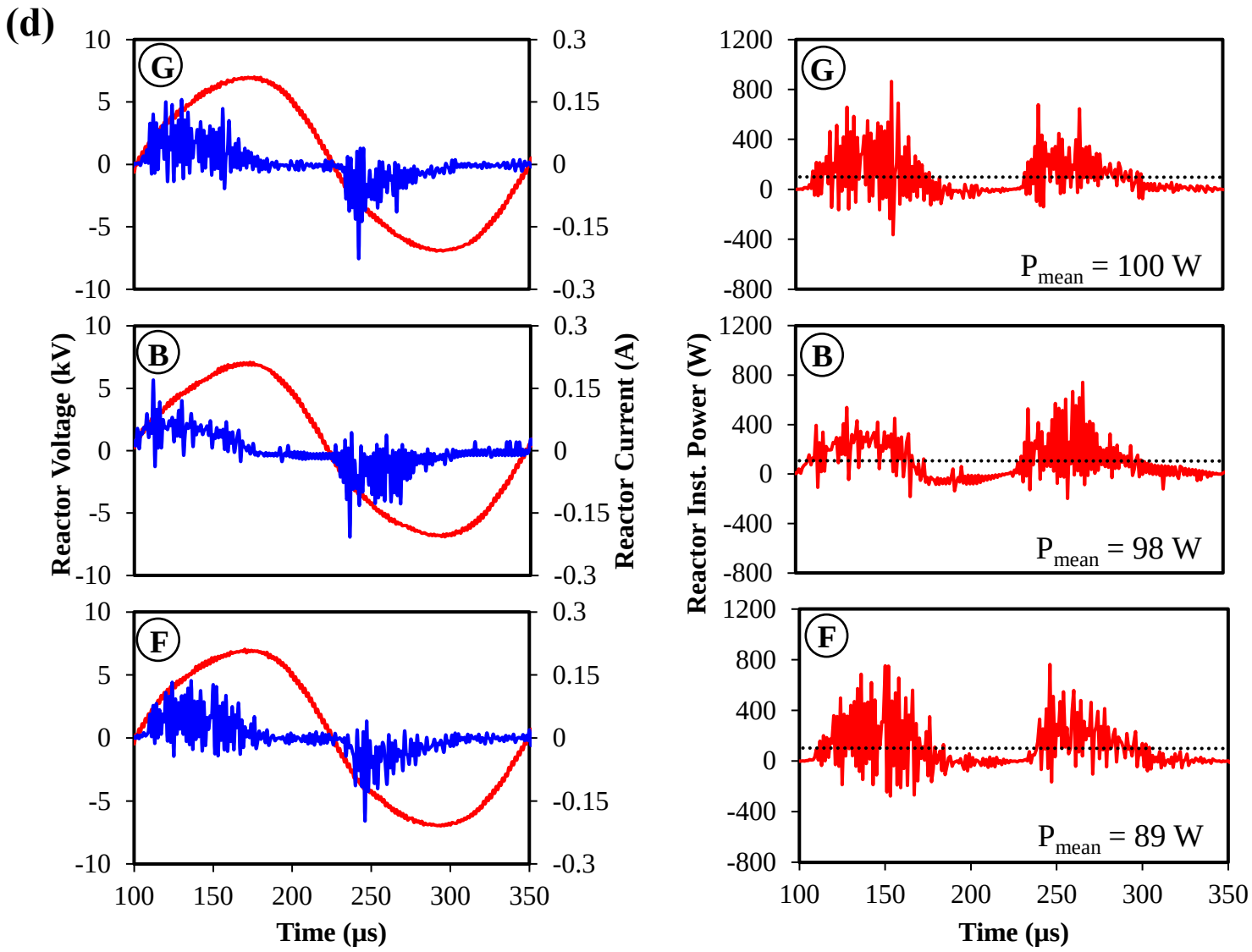
(d)
G
B
F
Reactor Voltage (kV)
Reactor Current (A)
Reactor Inst. Power (W)
Time (μs)
P mean = 100 W
P mean = 98 W
P mean = 89 W

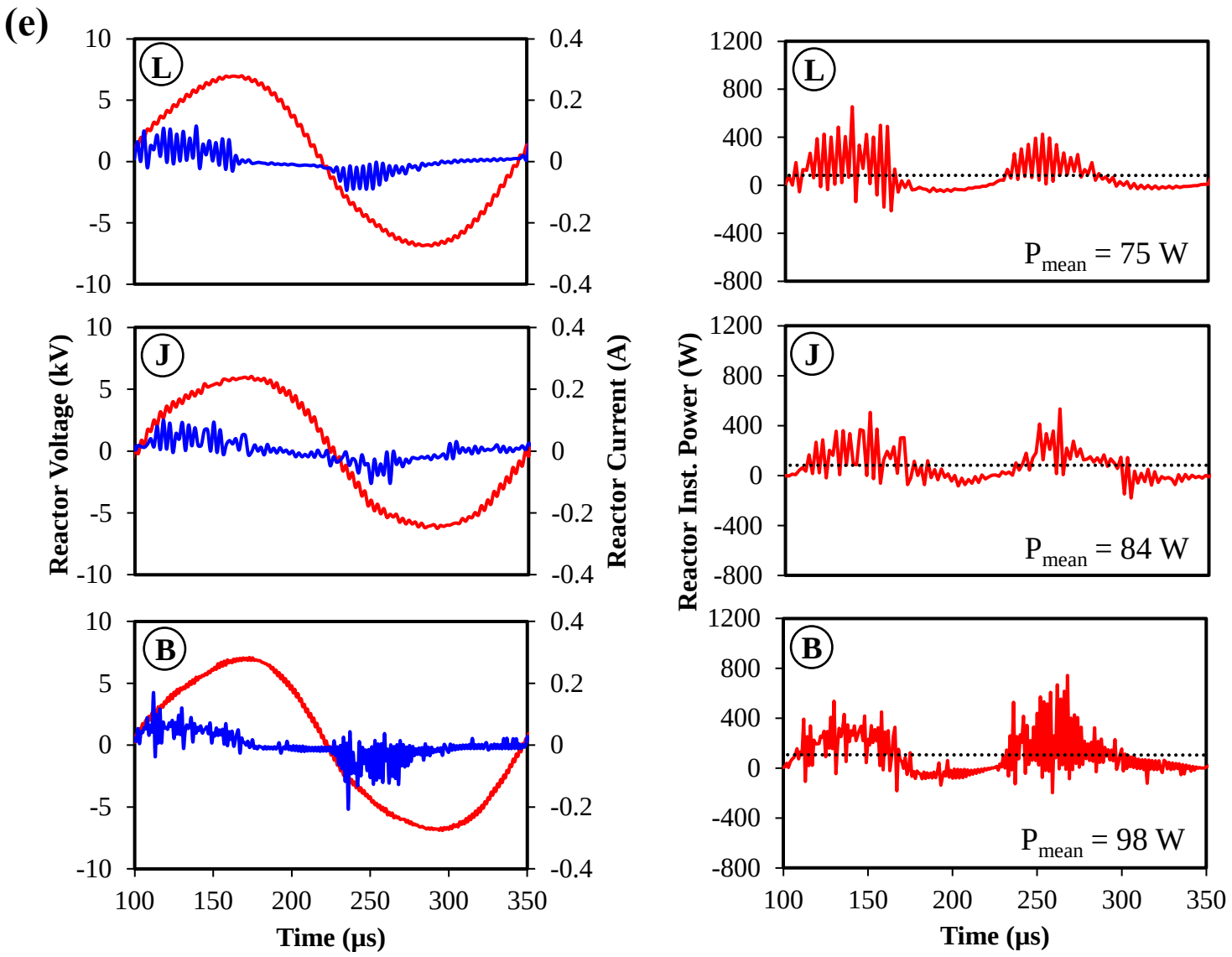
(e)
L
J
B
Reactor Voltage (kV)
Reactor Current (A)
Time (μs)
Reactor Inst. Power (W)
P mean = 75 W
P mean = 84 W
P mean = 98 W

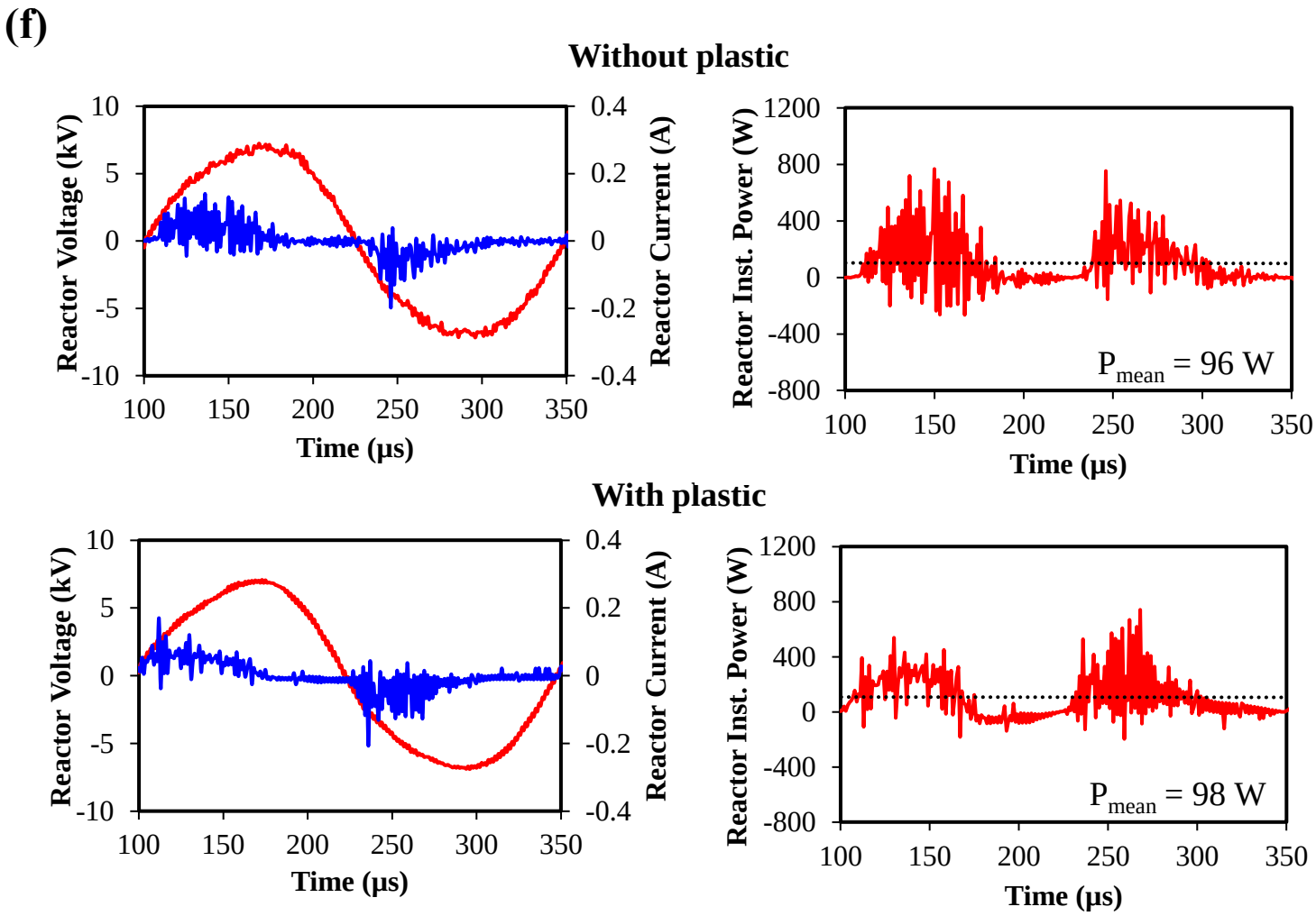

Figure S2. Plasma characterization including voltage, current, and instantaneous power as a function of time. The test conditions with different (a) voltages, (b) frequencies, (c) initial temperatures, (d) gas residence time, (e) oxygen concentration, and (f) without and with plastic inside the reactor. The condition IDs are given in **Table 1** of the main text. The dotted line indicates mean power.

(a)

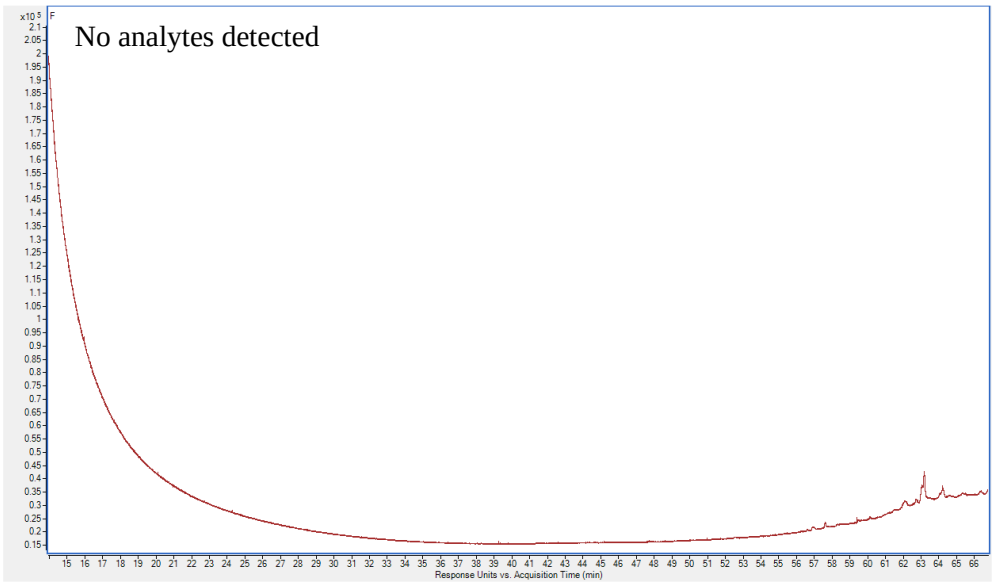

(b)

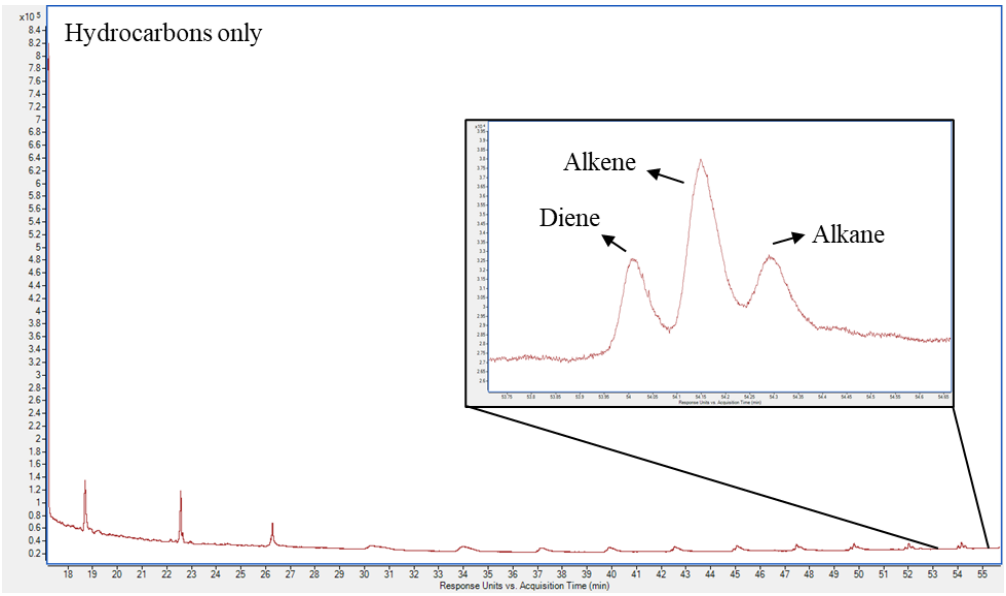

Figure S3. GC/MS chromatograms of **(a)** the PE sample preheated from room temperature to 350 °C in 4 min, and **(b)** condenser recovered products of the PE thermally converted at 350 °C under CO_2 atmosphere for 20 min.

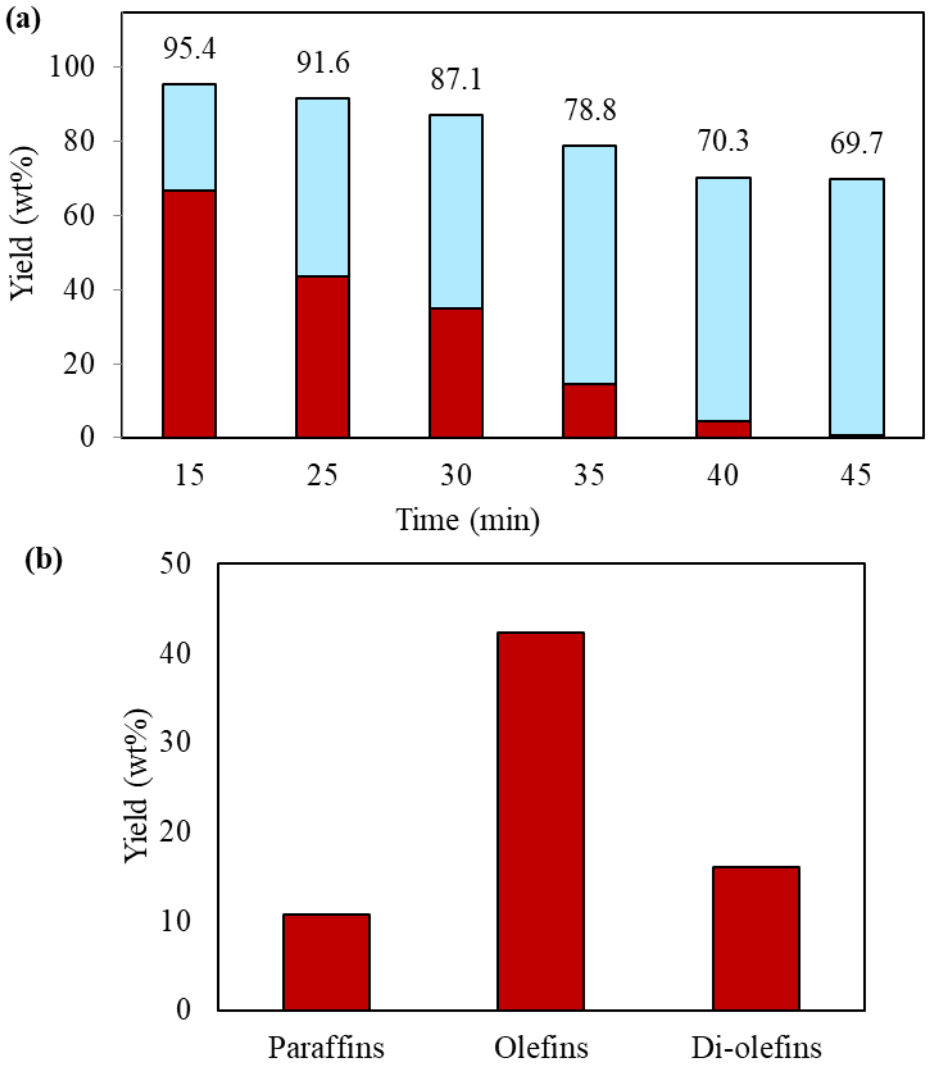

Figure S4. PE conversion by argon plasma. **(a)** Time-dependent liquid product and solid residue yields, and **(b)** liquids composition yields. Reaction conditions: f = 15 kV, V = 8 kHz, T_i = 350 °C, t_R = 13s, 45 min.

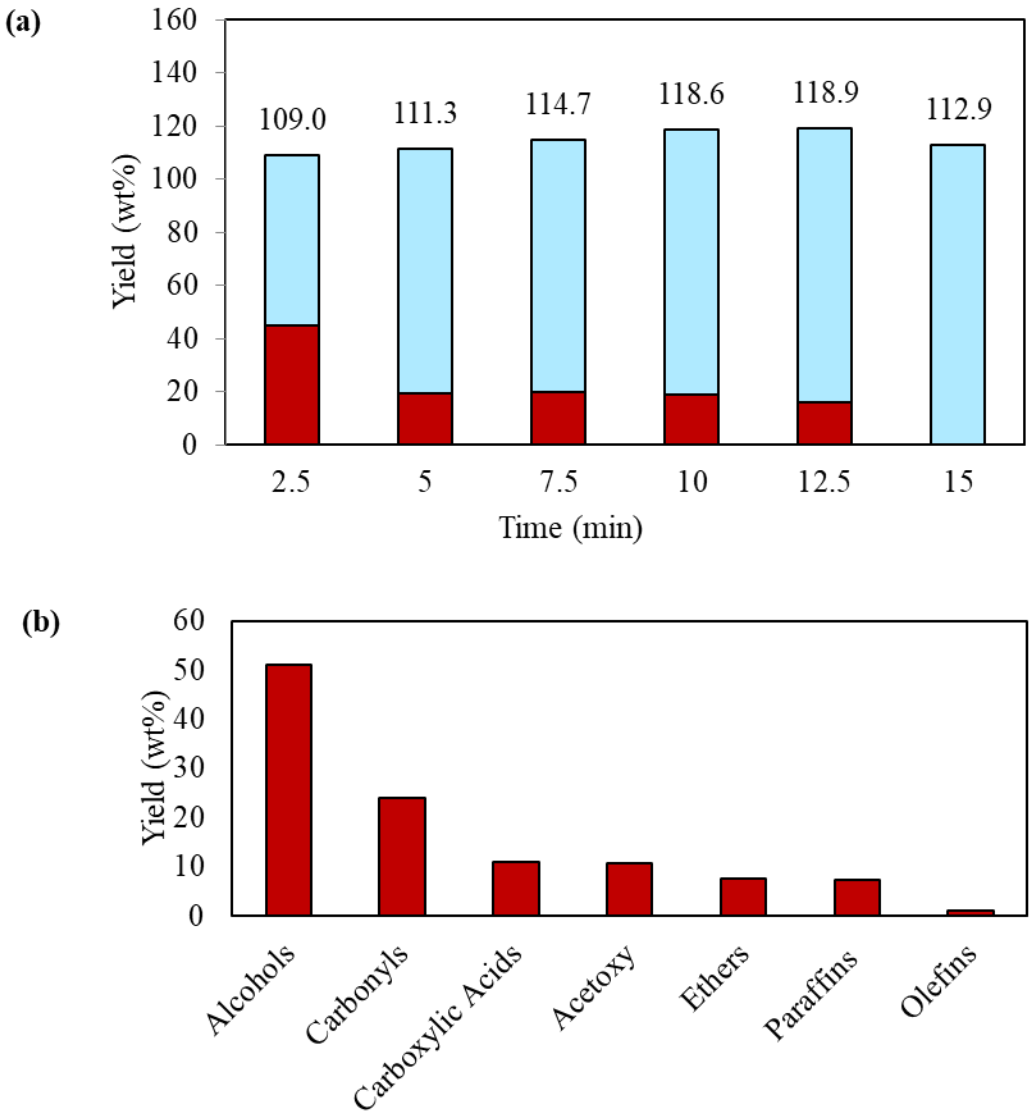

Figure S5. PE conversion by air plasma. **(a)** Time-dependent liquid product and solid residue yields, and **(b)** liquids composition yields. Reaction conditions: f = 15 kV, V = 8 kHz, T_i = 350 °C, t_R = 13s, time =15 min.

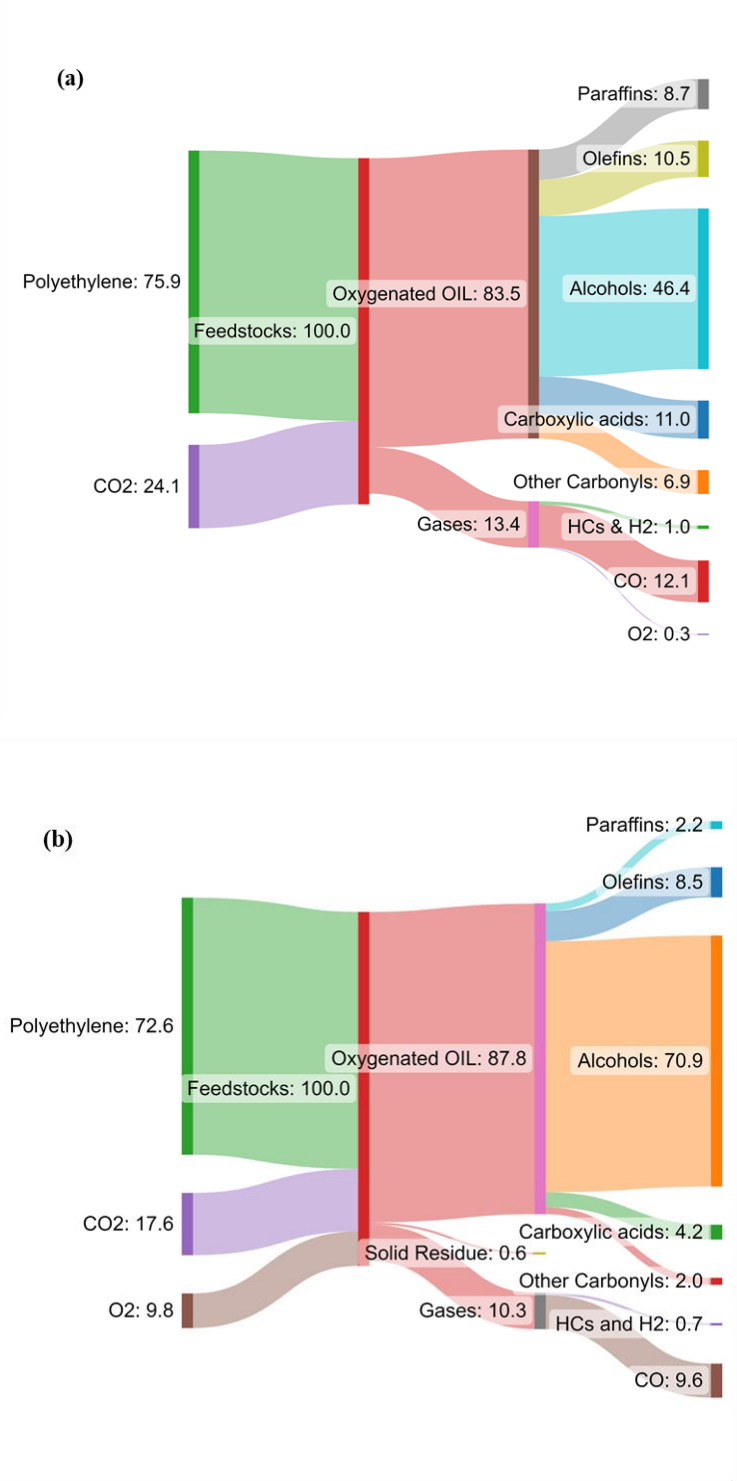

Figure S6. Sankey diagrams of plasma conversion pathways for PE: **(a)** CO_2 plasma for case G, and **(b)** CO_2/O_2 plasma for case J.

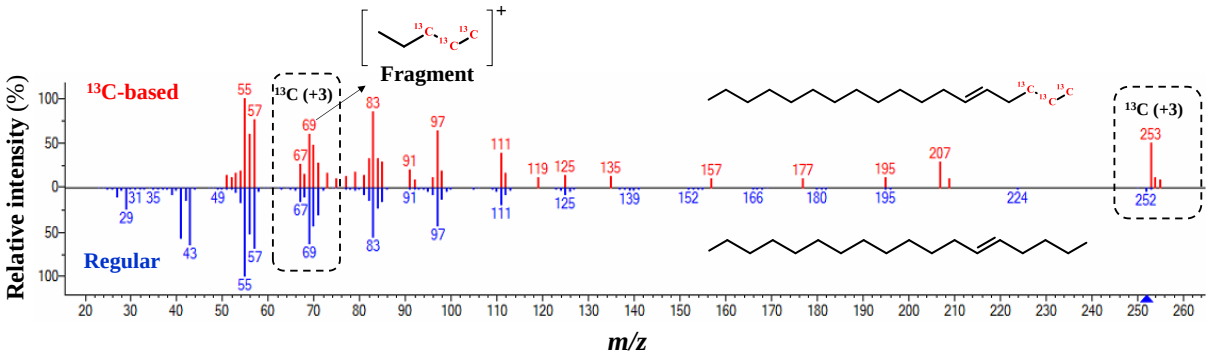

Figure S7. Mass spectra of 5-octadecene ($C_{18}H_{36}$, Mw = 252) compared between $^{13}CO_2$ plasma-based (upper) and regular (lower) molecules.

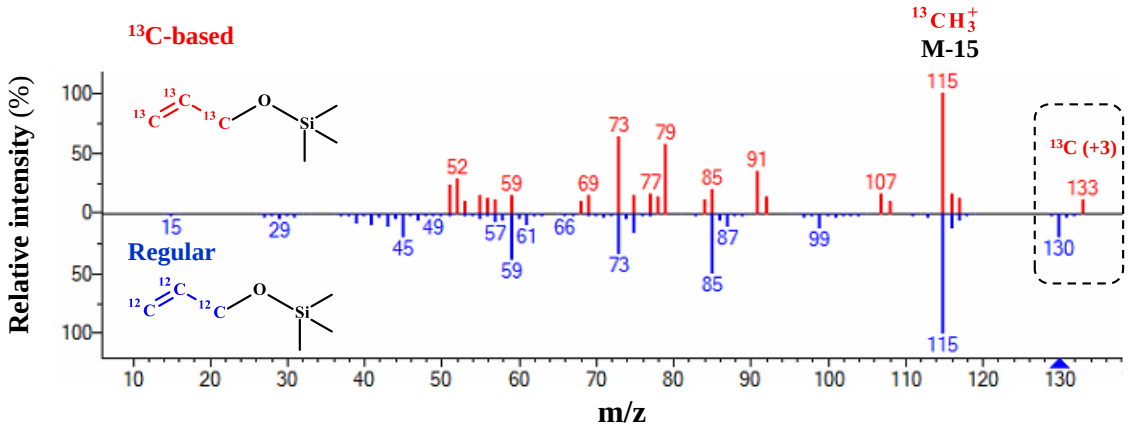

Figure S8. Mass spectra of allyl alcohol, TMS derivative ($C_6H_{10}OSi$, Mw = 130) compared between $^{13}CO_2$ plasma-based (upper) and regular (lower) molecules.

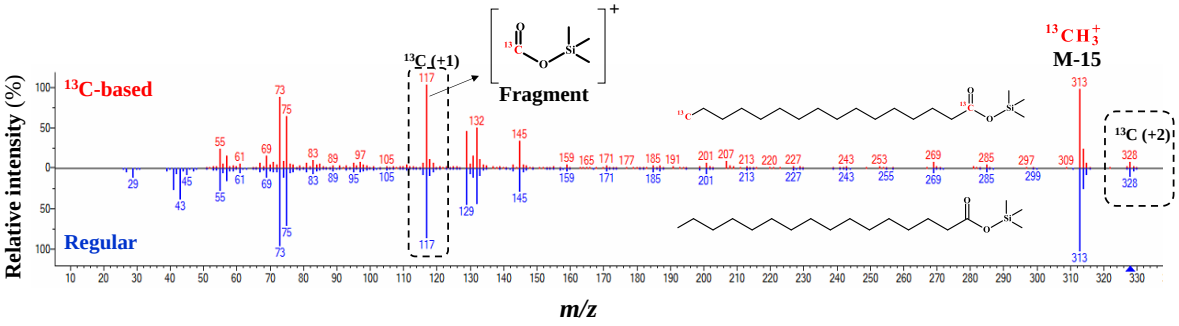

Figure S9. Mass spectra of palmitic acid, TMS derivative ($C_{19}H_{40}O_2Si$, Mw = 328) compared between $^{13}CO_2$ plasma-based (upper) and regular (lower) molecules.

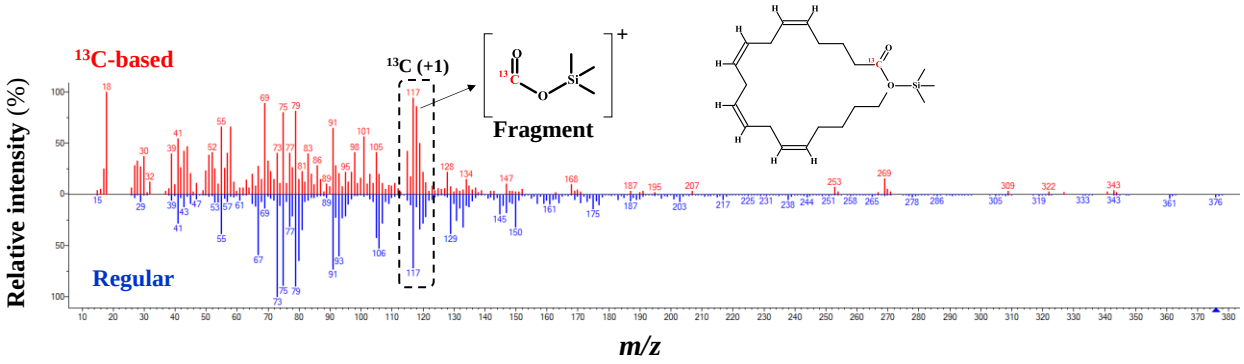

Figure S10. Mass spectra of Arachidonic acid, TMS derivative ($C_{23}H_{40}O_2Si$, Mw = 376) compared between $^{13}CO_2$ plasma-based (upper) and regular (lower) molecules.

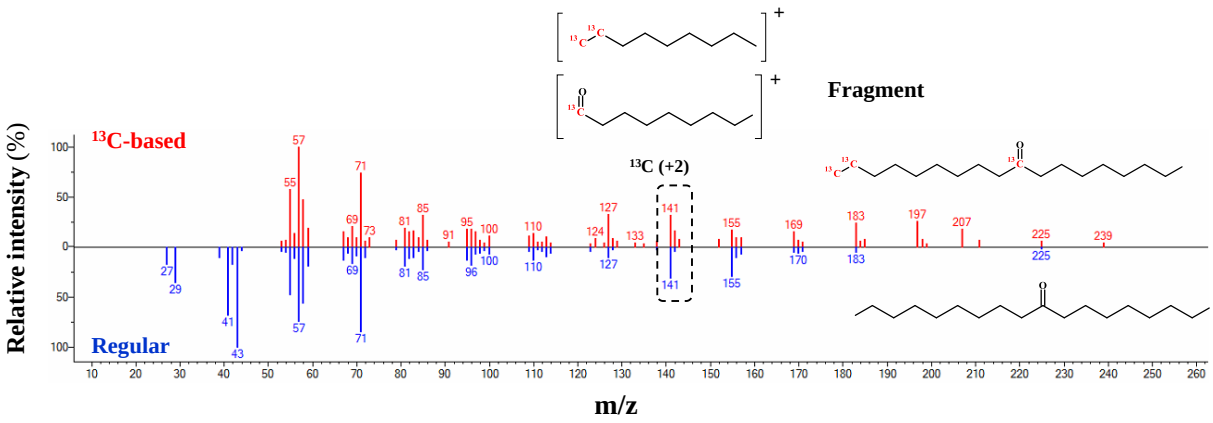

Figure S11. Mass spectra of 9-octadecanone ($C_{18}H_{36}O_1$, Mw = 268) compared between $^{13}CO_2$ plasma-based (upper) and regular (lower) molecules.

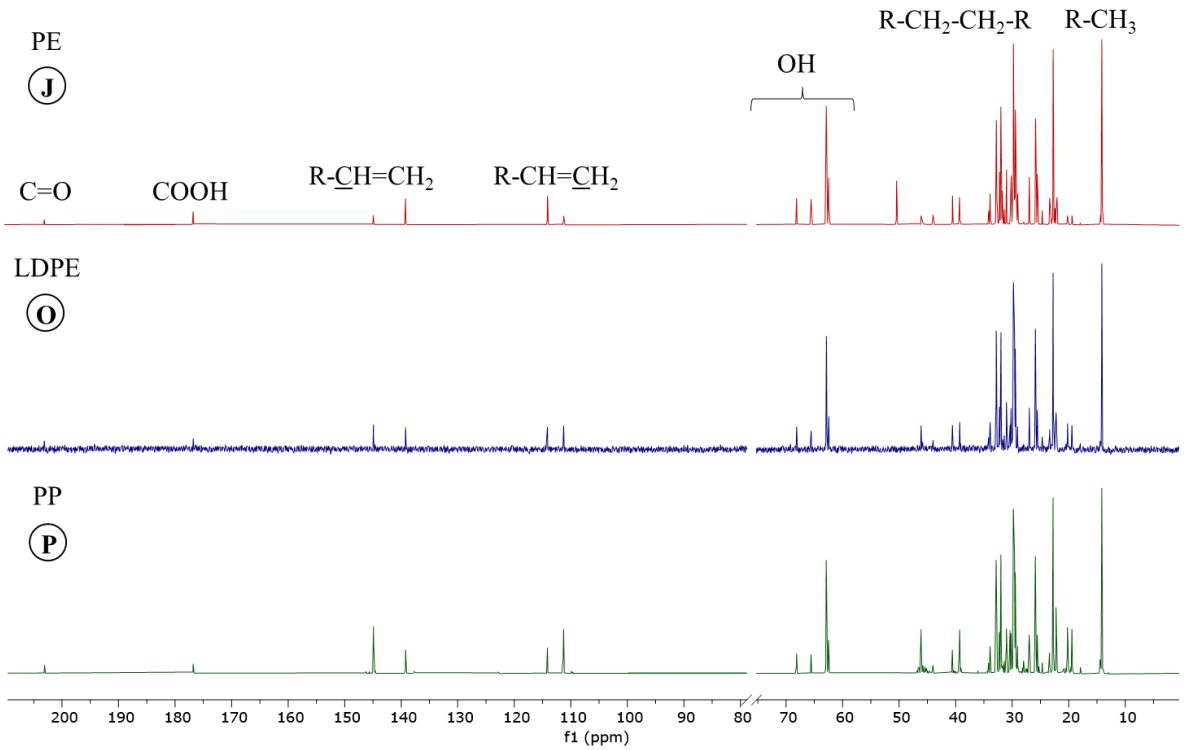

Figure S12. Quantitative ^{13}C NMR spectra of liquids obtained from conversion of different polyolefins under CO_2/O_2 plasma. The case numbers are indicated inside circles.

Figure S13. Post-consumer mixed PE (PC-PE) used in this work.

(a)

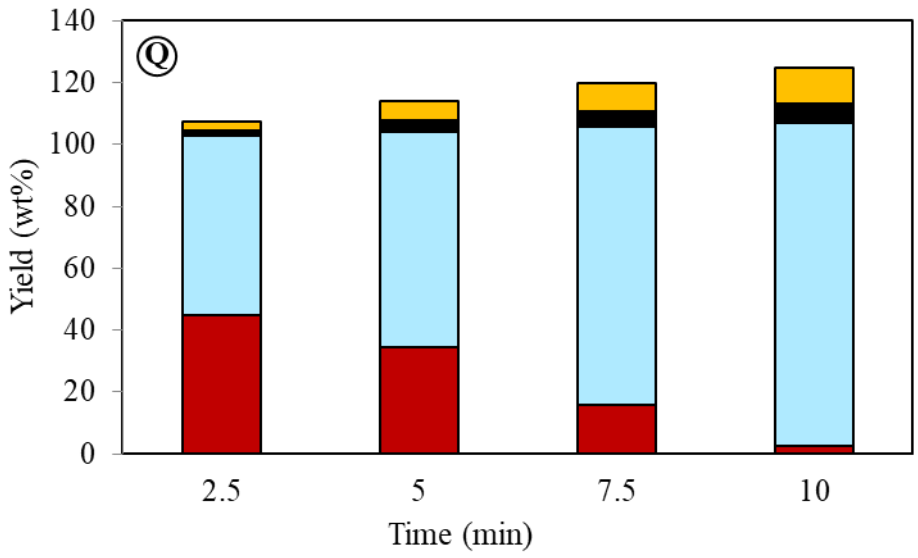
Q
Yield (wt%)
140
120
100
80
60
40
20
0
2.5
5
7.5
10
Time (min)

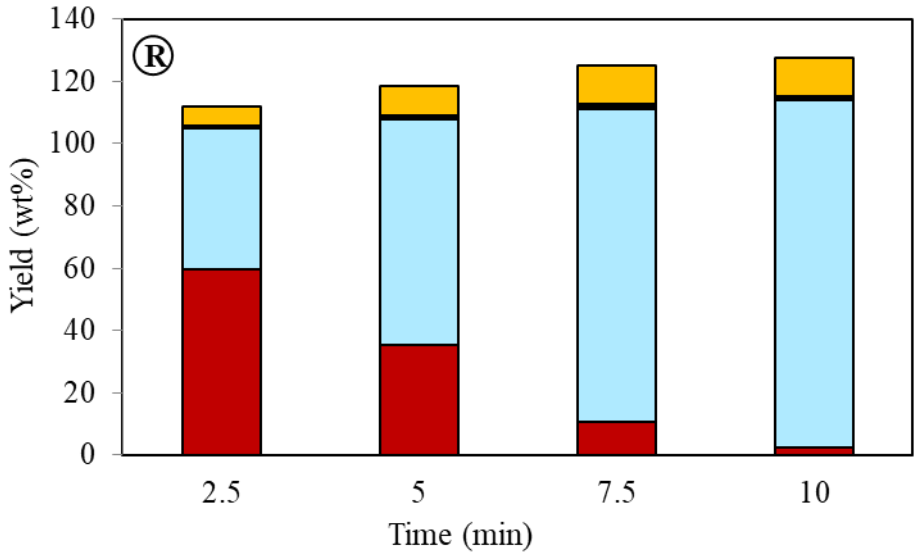
R
Yield (wt%)
140
120
100
80
60
40
20
0
2.5
5
7.5
10
Time (min)

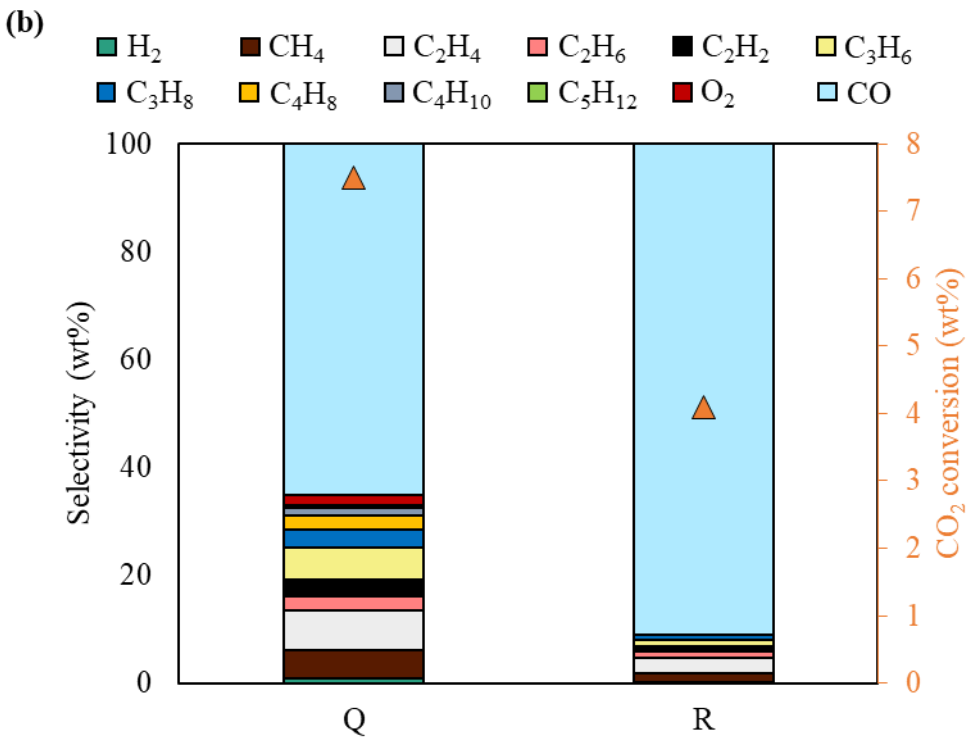

Figure S14. PC-PE conversion using CO_2 (case Q) and CO_2/O_2 plasma (case R). **(a)** Product yields per plastic mass, and **(b)** Gas products selectivity and CO_2 conversion.

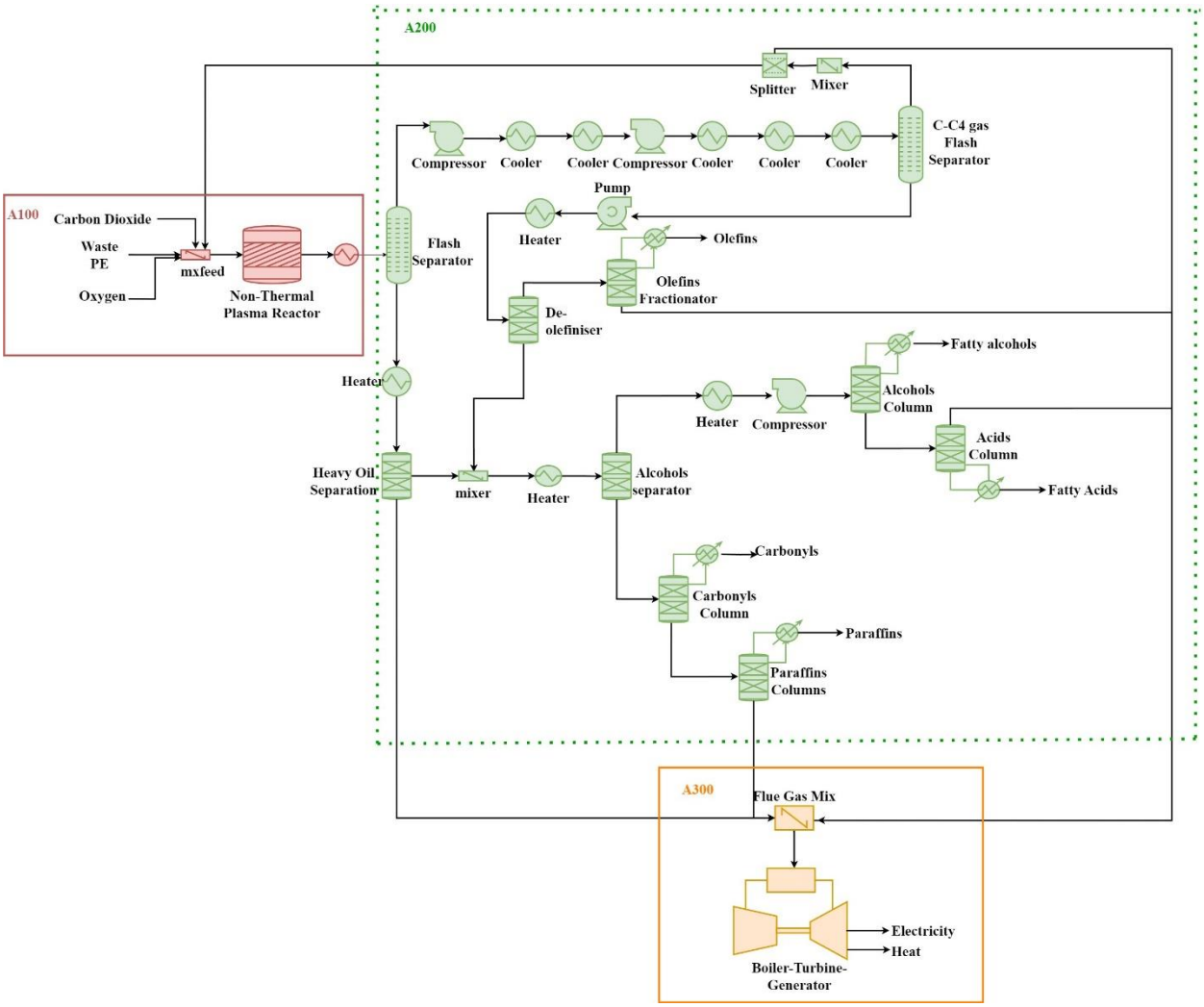

Figure S15. Process flow diagram for a commercial-scale plasma-based waste to fuel and chemicals facility. A100 denotes Plasma Deconstruction, A200 is Oil Fractionation and Recovery, and A300 is Heat Recovery/Steam Generation.

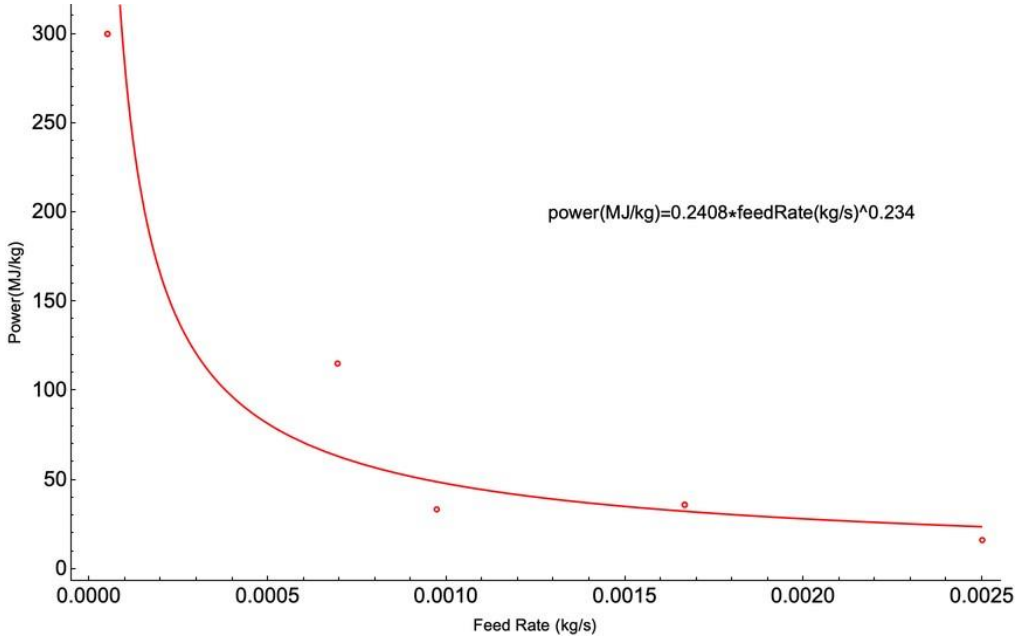

Figure S16. Plasma power versus reactor feed rate.

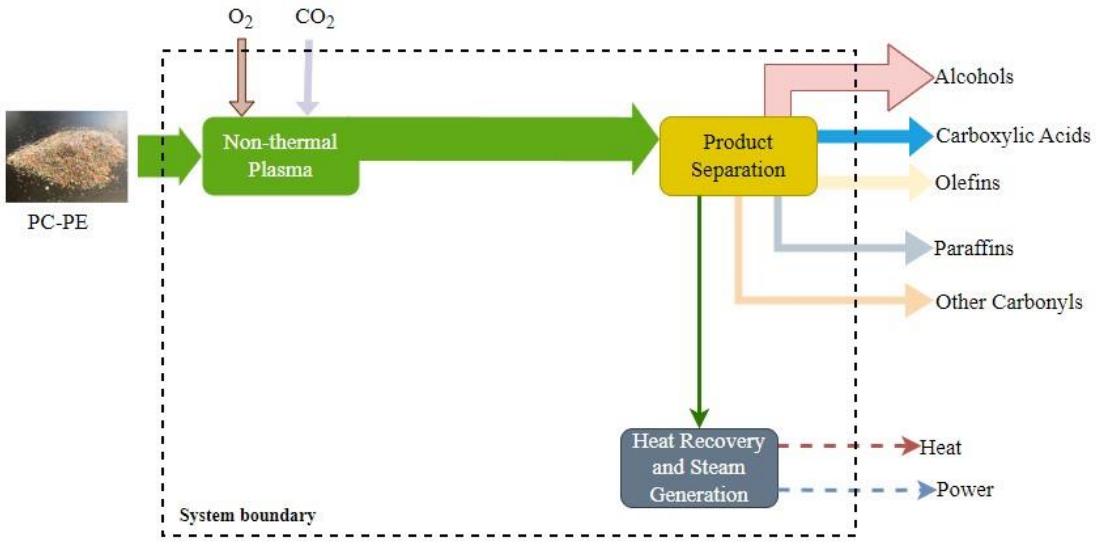

Figure S17. Lifecycle assessment system boundary for plasma-based plastic waste to fuels and chemicals facilities

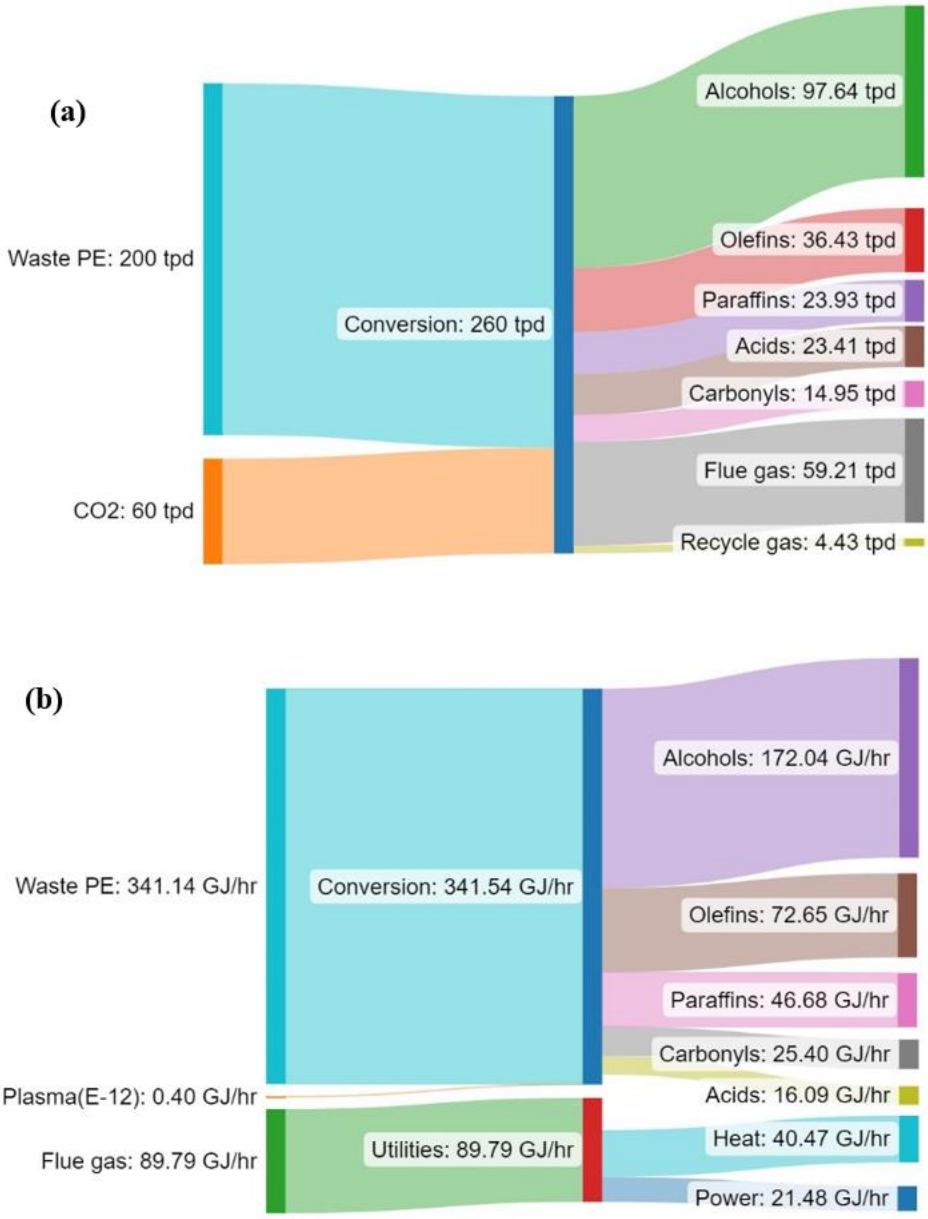

Figure S18. (a) Mass and **(b)** energy balance for plasma scenario 1 (CO_2 plasma) to alcohols and other chemicals.

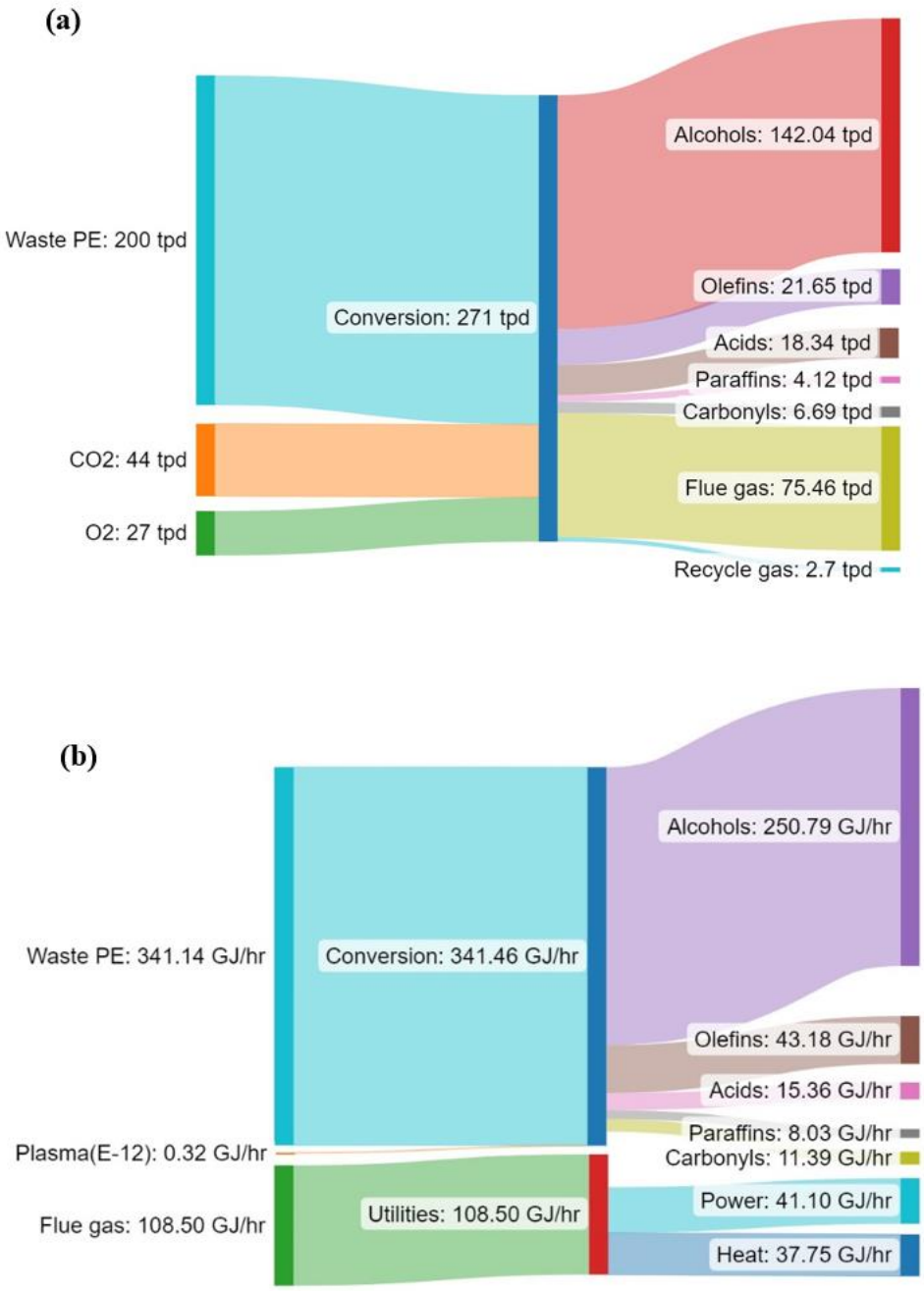

Figure S19. (a) Mass and **(b)** energy balance for scenario 2 (CO_2/O_2 plasma) to alcohols and other chemicals.

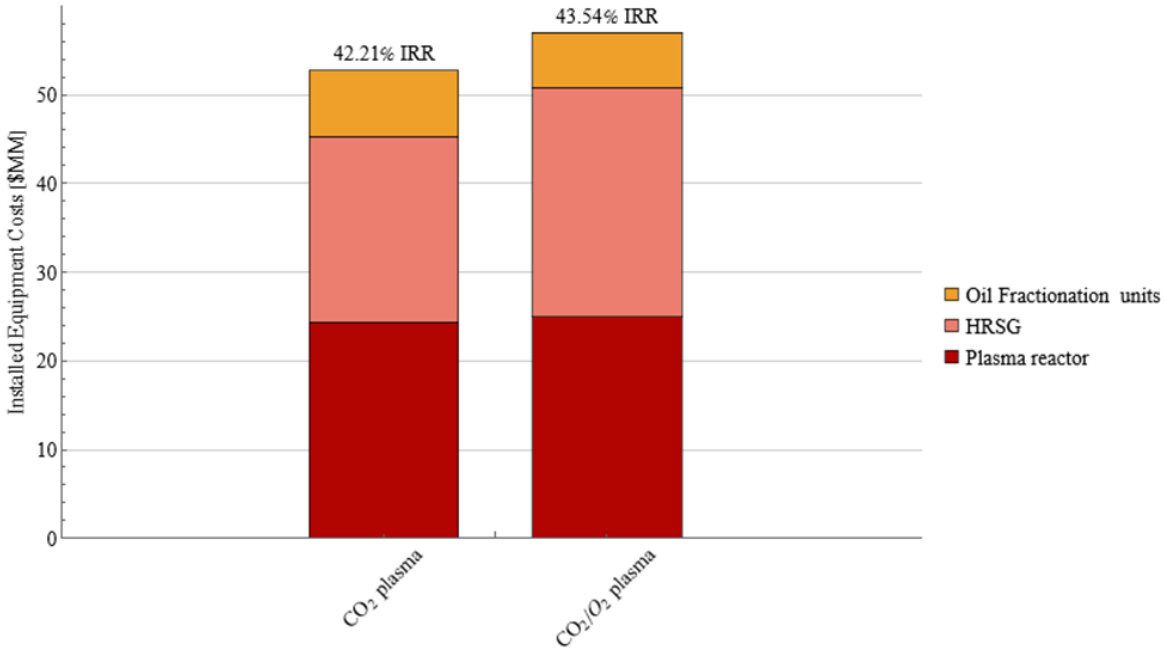

Figure S20. Installed equipment costs for two scenarios.

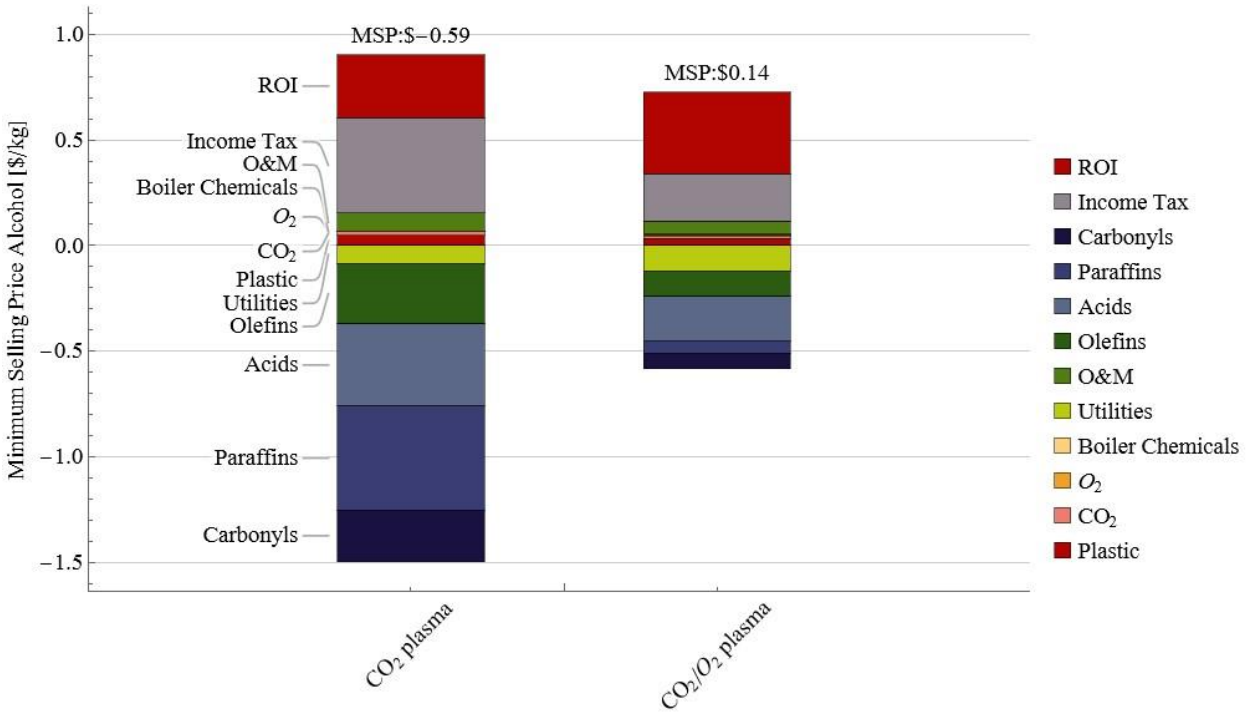

Figure S21. Contributions of operating costs and byproducts credits to the minimum selling price of alcohol.

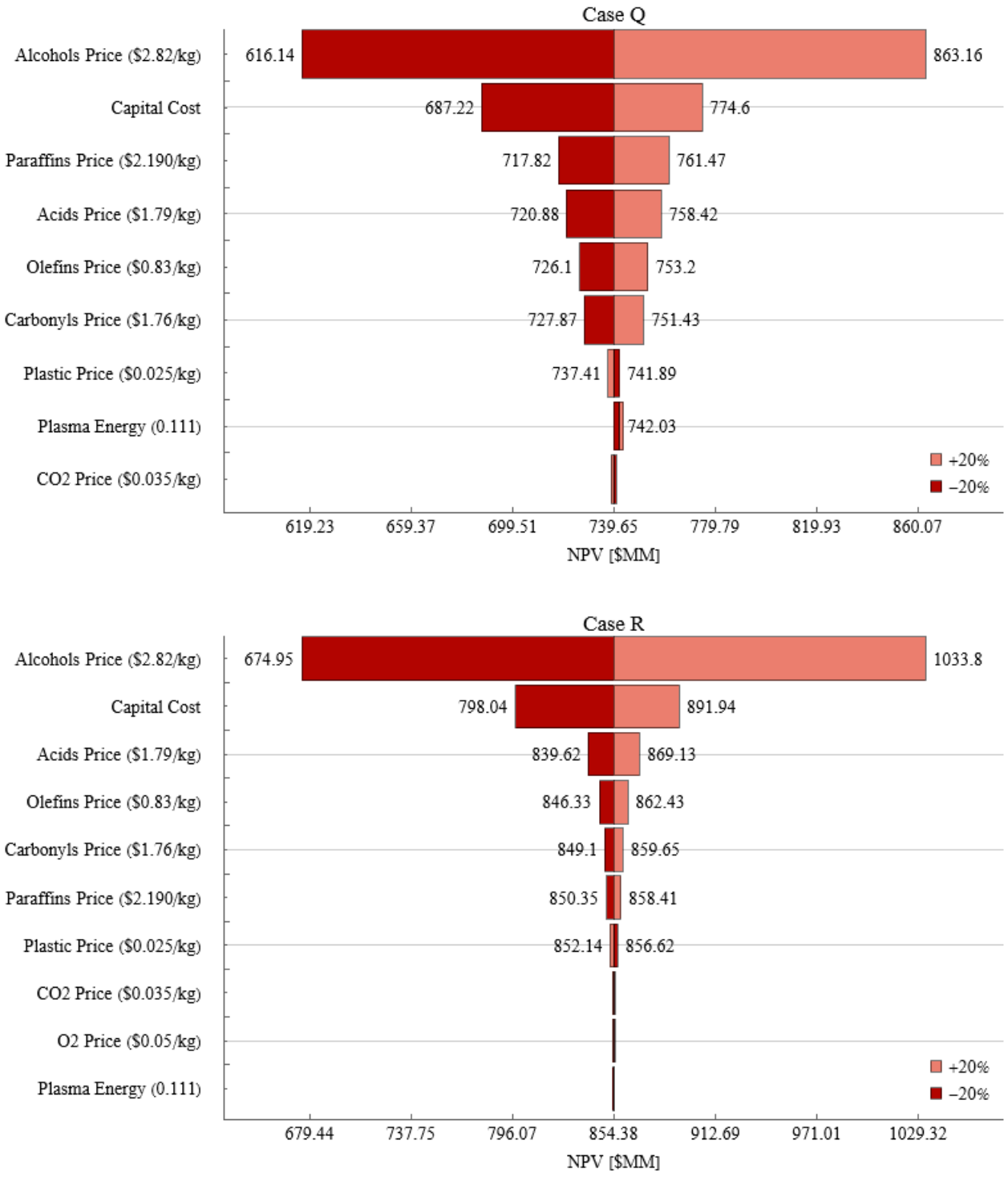

Figure S22. Sensitivity analysis of the net present value (NPV) to key techno-economic analysis parameters for two different scenarios.

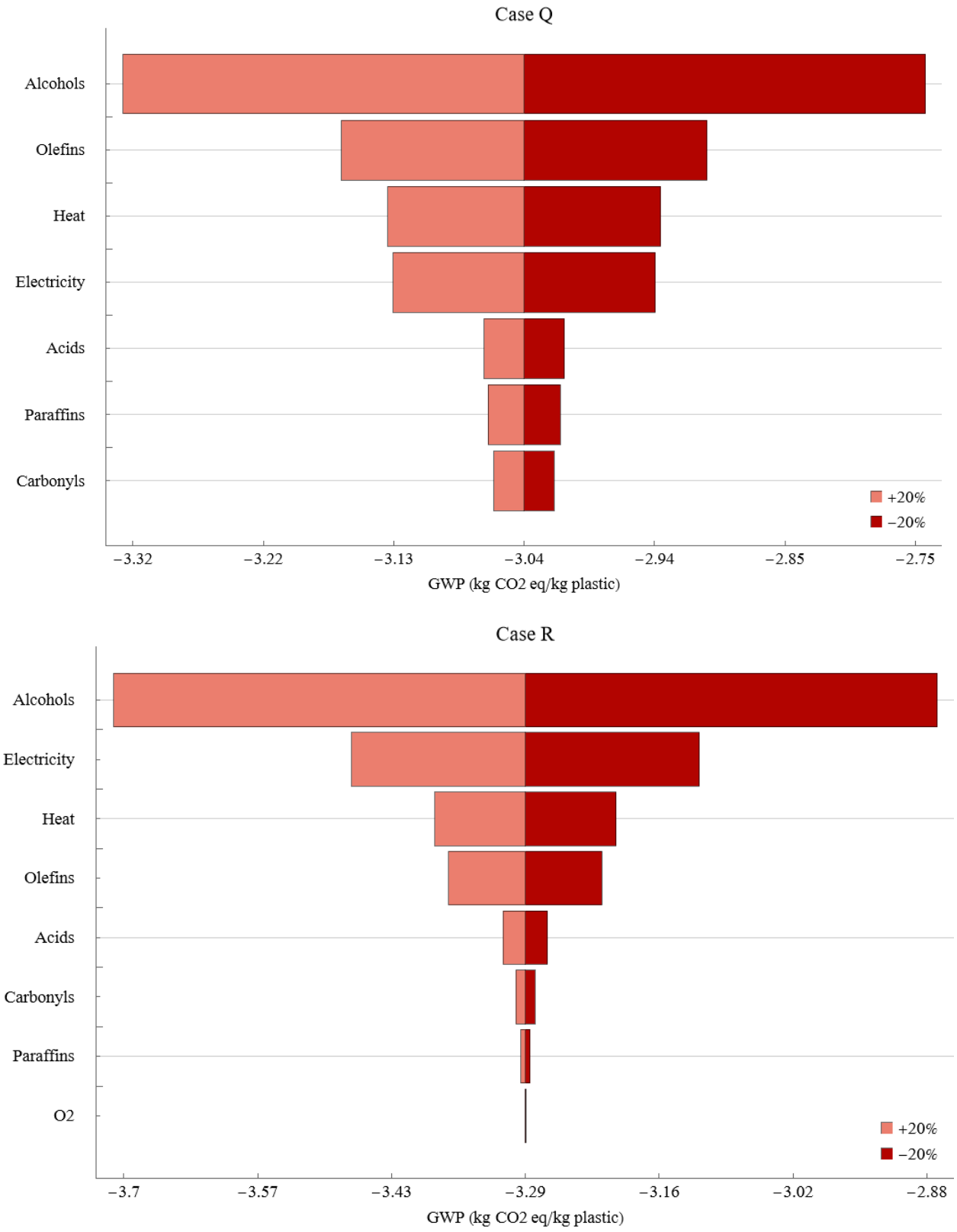

Figure S23. Sensitivity analysis of the Global Warming Potential (GWP) for plasma-based plastic waste recycling to fuels and chemicals for scenario 1 and scenario 2.

Supplementary Tables

Table S1. Average internal gas temperature in the plasma reactor and plasma power for PE conversion using different reaction conditions.

Case*	Average Power (W)	Average T (°C)
A	44	252
B	98	339
C	138	396
D	96	329
E	118	359
F	89	299
G	100	353
H	90	266
I	111	395
J	84	344
K	77	367
L	75	370

* Refer to main manuscript Table 1 for nomenclature.

Table S2. Reproducibility of the experiment using PE conversion by case B and G of CO_2 plasma and case J of CO_2/O_2 plasma as an example.

Case	Trial #	PE mass (g)	Liquid mass (g)	Liquid yield (%)	CO_2 conversion (%)
B	1	0.1532	0.1695	110.6	6.25
	2	0.1481	0.1653	111.6	6.3
	3	0.1528	0.1712	112	6.27
	Average (%)			111.4	6.27
	Standard error (%)			±0.7	±0.03
G	1	0.1506	0.167	110.9	7.49
	2	0.1534	0.168	109.5	7.47
	3	0.1515	0.1656	109.3	7.42
	Average (%)			109.9	7.46
	Standard error (%)			±0.9	±0.04
J	1	0.153	0.1826	119.3	5.52
	2	0.1519	0.1834	120.7	5.58
	3	0.1528	0.1863	121.9	5.6
	Average (%)			120.7	5.58
	Standard error (%)			±1.3	±0.04

Table S3. Moisture content of liquid products obtained from PE or PC-PE conversion using CO_2 plasma or CO_2/O_2 plasma.

Moisture (%)	PE			PC-PE
	CO_2		CO_2/O_2	CO_2/O_2
	B	G	J	R
	0.2	0.6	0.5	0.7

Table S4. ^{13}C NMR-based functional group selectivity of liquids produced from PE conversion using CO_2 (case G) and CO_2/O_2 (case J) plasma.

Functional Group	Selectivity (%)	
	CO_2	CO_2/O_2
Alcohols	54.3	74.9
Carboxylic acids	16.2	5.1
Other oxygenated compounds	3.3	1.6
Hydrocarbons	26.2	18.5

Table S5. Mass closures of plasma-based co-conversion of plastics and CO_2, including all reactants and measured products.

Plastic	Plasma	Case	Gas (%)	Liquid (%)	Solid Residue (%)	Total (%)
PE	CO_2	G	13.4	83.5	0.0	96.9
PE	CO_2/O_2	J	10.4	87.7	0.6	98.7
PC-PE	CO_2	Q	14.1	80.7	2	96.8
PC-PE	CO_2/O_2	R	9.8	82.1	1.8	93.7

* The gas, liquid and solid residue yields are calculated based on the total reactant masses, which are PE and converted CO_2 for the CO_2 plasma case, and PE, and converted CO_2 and O_2 for the CO_2/O_2 plasma cases.

Table S6. *m/z* peak intensity ratios of palmitic acid, TMS derivative, and arachidonic acid, TMS derivative for their regular molecules and $^{13}CO_2$ plasma-based molecules.

Entry	*m/z*	Regular	$^{13}CO_2$ plasma-based
Palmitic acid, TMS derivative			
1	118/117	9.8%	10.3%
2	119/117	4.0%	5.5%
3	314/313	24.1%	24.2%
4	315/313	6.4%	6.1%
5	329/328	27.3%	29.1%
6	330/328	7.9%	13.4%
Arachidonic acid, TMS derivative			
7	118/117	14.7%	91.1%
8	119/117	43.0%	53.2%

Table S7. *m/z* peak intensity ratios of 9-octadecanone for the regular molecule and $^{13}CO_2$ plasma-based molecule.

Entry	*m/z*	Regular	$^{13}CO_2$ plasma
1	142/141	13%	50.9%
2	143/141	0%	24.5%

Table S8. ^{13}C NMR-based functional group selectivity of liquids produced from LDPE and PP using CO_2/O_2 plasma (cases O and P).

Functional Group	Feedstock	
	LDPE	PP
Alcohols	72.6	69.8
Carboxylic acids	2.6	3.3
Other oxygenated compounds	0.4	3.6
Hydrocarbons	24.4	23.3

Table S9. Economic assumptions

Parameters	Value
Plant financing by equity/debt	40%/60%
Plant lifetime	20 years
Operating days	333 days
Income tax rate	21%
Financing interest rate	7%
Term for debt financing	10 years
Plant capacity	200 MT/day of plastic waste
Depreciation period	7-year MACRS schedule
Working Capital	5% fixed capital investment
LANG factor	5
Construction period (spending schedule)	2 years (40% Y1, 60% Y2)
Startup time	6 months
Plant salvage value	No value
Revenue and costs during startup	50% of normal revenue 75% of the normal variable cost 100% of fixed cost

Table S10. Operating cost parameters and assumptions

Parameters	Value	Units	Source
Materials			
PC-PE	25.05	$/MT	*10,13*
O_2	0.05	$/kg	*26*
CO_2	35	$/MT	*14,15*
Products credits			
Paraffins	2.19	$/kg	*21*
Olefins	0.83	$/kg	*22*
Fatty alcohols	2.82	$/kg	*19*
Fatty acids	1.79	$/kg	*20*
Carbonyls	1.76	$/kg	*23*
Utilities			
Electricity	0.0701	$/kWh	*27*
Cooling water	0.035	$/$m^3$	*16*
Process water	0.23	$/$m^3$	*17*
Chilled water	0.0225	$/kWh	*18*
Wastewater treatment	0.022	$/gal	*12*
Fixed charge			
Labor cost	$2,255,473	$/year	*12*
Insurance	0.5% FCI		
Property tax	0.1% FCI		
Depreciation	MACRS 7		
Fringe benefits	4% labor cost		
Equipment maintenance	0.3% FCI		
Operating supplies	20% labor cost		
Administrative cost	0.5% FCI		

Table S11. Emission factors from OpenLCA

Emission factors	**Units**	**kg CO2-Eq**	**Process OpenLCA**
Waste collection*a	kg	0.225	Market for waste polyethylene, for recycling, unsorted
Waste treatment*a	kg	0.167	Treatment of waste polyethylene
Oxygen	kg	0.575	Oxygen, liquid
Avoided emissions			
Alcohols	kg	2.958	Fatty alcohol production, petrochemical
Acids	kg	1.233	Acetic acid production, petrochemical
Carbonyls	kg	1.453	Acetaldehyde production, petrochemical
Paraffin	kg	1.169	Lubricating oil
Olefins	kg	3.611	Propylene glycol, liquid
Electricity	MJ	0.649	Electricity, high voltage
Heat	MJ	0.102	Heat, from steam, in chemical industry

*a Waste collection and treatment are assumed to have zero-burden in the recycling system boundary and are shown here to illustrate their relative impact

Table S12. Summary of environmental impacts of all scenarios*

Scenarios	Scenario 1	Scenario 2	Scenario 3	Scenario 4
GWP	-3.07	-3.29	-3.11	-3.33
Acid.	-0.64	-0.7	-0.64	-0.71
Eutroph.	-3.49E-03	2.13E-02	-3.50E-03	2.13E-02
Ecotox.	-1.07	-1.05	-1.08	-1.06
O_3 dep.	-5.54E-07	7.93E-05	-5.55E-07	7.94E-05
Photo oxi.	-6.93E-03	4.73E-02	-6.98E-03	4.72E-02
Carcinog.	-3.72E-03	4.06E-02	-3.74E-03	4.06E-02

**GWP* = Global Warming Potential in kg_{CO2}/kg_{PE}; *Acid.* = acidification impact in moles of H^+Eq./kg_{PE}; *Eutroph.* = eutrophication impact in kg N/kg_{PE}; *Ecotox.* = ecotoxicity impact in kg 2,4-D,e/kg_{PE}; *O_3 dep.* = ozone depletion impact in kg CFC-11-e/kg_{PE}; *Photo oxi.* = photochemical oxidation impact in kg NOx-e/kg_{PE}; *Carcinog.* = carcinogenic impact in kg benzene-e/kg_{PE}.

Supplementary References

1. R. Wang, Y. Luo, H. Jia, J. R. Ferrell and H. Ben, *RSC Adv.*, 2020, 10, 25918–25928.
2. R. Partington, J. Clarkson, J. Paterson, K. Sullivan and J. Wilson, *J. Anal. Sci. Technol.*, 2020, 11, 42.
3. R. J. Speight et al., *Solid State Nucl. Magn. Reson.*, 2011, 39, 58–64.
4. O. Olafasakin, J. Ma, S. L. Bradshaw et al., *Waste Manag.*, 2023, 166, 368–376.
5. Y. Cortes-Peña, D. Kumar, V. Singh and J. S. Guest, *ACS Sustain. Chem. Eng.*, 2020, 8, 3302–3310.
6. P. N. Dave and A. K. Joshi, *J. Sci. & Ind. Research*, 2010, 69, 177-179.
7. C. Ducharme, N. J. Themelis and M. J. Castaldi, *Technical and economic analysis of Plasma-assisted Waste-to-Energy processes*, 2010.
8. T. Maczka, M. Wnukowski, E. Sliwka and L. Niedzwiecki, *Pilot installation for the Thermal Plasma Treatment of Plastic Wastes*, 2013.
9. S. Kwon and S. kyun Im, *Energy Convers. Manag.*, 2022, 251, 114978.
10. O. Olafasakin, J. Ma, V. Zavala, R. C. Brown, G. W. Huber and M. Mba-Wright, *Energy Fuels*, 2023, 37, 15832–15842.
11. V. Cappello, P. Sun, G. Zang et al., *Green Chem.*, 2022, 24, 6306–6318.
12. D. Humbird, R. Davis, L. Tao et al., NREL Report, 2011, NREL/TP-5100-47764.
13. U. R. Gracida-Alvarez, O. Winjobi, J. C. Sacramento-Rivero and D. R. Shonnard, *ACS Sustain. Chem. Eng.*, 2019, 7, 18254–18266.
14. Do TN, You C, Kim J. Energy Environ Sci. 2022;15:169-184.
15. Kim J, Johnson TA, Miller JE, Stechel EB, Maravelias CT. Energy Environ Sci. 2022;15:169-184.
16. INTRATEC, Cooling Water Cost, available at: https://www.intratec.us/products/water-utility-costs/commodity/cooling-water-cost, accessed November 10, 2023.
17. INTRATEC, Process Water Cost, available at: https://www.intratec.us/products/water-utility-costs/commodity/process-water-cost, accessed November 10, 2023.
18. INTRATEC, Chilled Water Cost, available at: https://www.intratec.us/products/water-utility-costs/commodity/chilled-water-cost, accessed November 10, 2023.
19. ChemAnalyst, Fatty Alcohol Price Trend and Forecast. Available at https://www.chemanalyst.com/Pricing-data/fatty-alcohol-1084 (accessed Nov 10, 2023).

20. ChemAnalyst, Fatty Acid Price Trend and Forecast. Available at https://www.chemanalyst.com/Pricing-data/fatty-acid-1257 (accessed Nov 10, 2023).

21. ChemAnalyst, Paraffin Wax Price Trend and Forecast, available at: https://www.chemanalyst.com/Pricing-data/paraffin-wax-1205, accessed November 10, 2023.

22. ChemAnalyst, Linear Alpha Olefin Price Trend and Forecast, available at: https://www.chemanalyst.com/Pricing-data/linear-alpha-olefin-1103, accessed November 10, 2023.

23. ChemAnalyst, Paraformaldehyde Price Trend and Forecast, available at: https://www.chemanalyst.com/Pricing-data/paraformaldehyde-pfa-1195, accessed November 10, 2023.

24. openLCA Modeling Suite, GreenDelta GmbH, Berlin, Germany, 2023, available at: https://www.openlca.org/openlca/, accessed November 30, 2023.

25. Djuric Ilic D, Eriksson O, Ödlund L. J Clean Prod. 2018;180:1-2.

26. B. Adhikari, C. J. Orme, J. R. Klaehn and F. F. Stewart, *Sep. Purif. Technol.*, 2021, 268, 118703.

27. W. Li, Q. Dang, R. Smith, R. C. Brown and M. M. Wright, *ACS Sustain. Chem. Eng.*, 2017, 5, 1528–1537.